INORGANIC CHEMISTRY

FRONTIERS

Accepted Manuscript

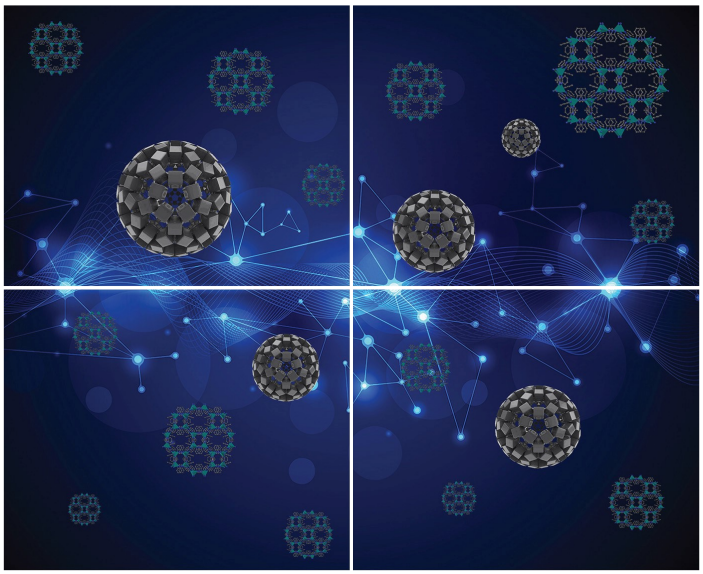

This article can be cited before page numbers have been issued, to do this please use: A. Brison, G. Pratviel and C. Hureau, *Inorg. Chem. Front.*, 2026, DOI: 10.1039/D6QI00446F.

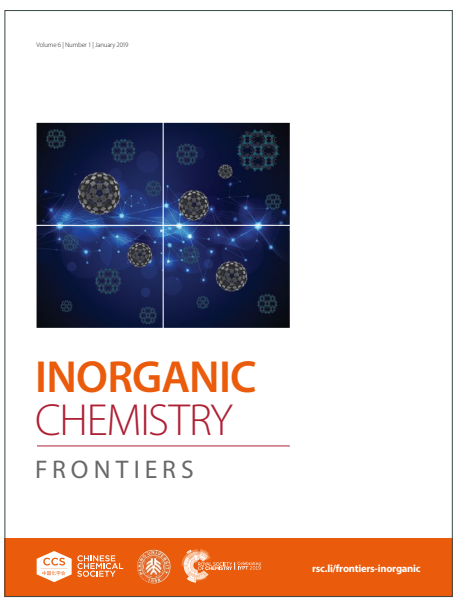

View Article Online
DOI: 10.1039/D6QI00446F

Biphasic modulation of Aβ(1–40) self-assembly by porphyrins: effects of concentration and structural variation

Adèle Brison[1], Geneviève Pratviel[1], Christelle Hureau[1*]

[1] Univ Toulouse, CNRS, LCC, Toulouse, France

Corresponding author: christelle.hureau@lcc-toulouse.fr

DOI: 10.1039/D6QI00446F

Abstract

Aβ peptides self-assemble into senile plaques, a hallmark of Alzheimer's disease (AD). The search for compounds able to modulate peptide self-assembly still await molecular and structural insights. In the present work, we have investigated a series of cationic porphyrins. By monitoring the kinetics of peptide self-assembly by thioflavin T (ThT) fluorescence and by imaging the assemblies formed using TEM and AFM, we observed : (i) first, some of them accelerate Aβ(1-40) self-assembly with an extent that increases with the porphyrin concentration. For the others, a relapse of the kinetic rates is observed above a concentration threshold (noted C_M) that is porphyrin-dependent. The biphasic modulation thus observed has not been reported so far in case of porphyrins; (ii) second, the porphyrins decrease the level of Aβ(1-40) fibrils formed as their concentration increases. The interactions between the porphyrins and the Aβ(1-40) have been thoroughly characterized by UV-visible, NMR, and fluorescence spectroscopies. The obtained data support a structure-dependent model involving π-stacking, electrostatic and hydrophobic interactions, responsible for the different effects of the porphyrins on the Aβ(1-40) self-assembly.

Introduction

Amyloid-related diseases, such as Alzheimer's Disease (AD), Parkinson's disease, Type-II diabetes, all rely on a common mechanism involving the self-assembly of a disease-specific intrinsically disordered peptide.[1-5] In the case of AD, the peptide at play is the Amyloid-β (Aβ). Its overproduction and its accumulation as aggregates and fibrils in senile plaques is one of the hallmarks of AD. Aβ self-assembly is currently regarded as a major contributor to the neuronal damage and memory impairment observed in the AD brain.[6-10]

Aβ is a 40-42 amino-acid residues peptide built on three main domains: (i) the N-terminal part rich in histidine (His) and carboxylate-containing residues and where metal ions can bind,[11, 12] (ii) the regions involved in β-strand formation that gather the central hydrophobic core (CHC) and the C-terminal part of the peptide, and (iii) the residues involved in the formation of a turn (Scheme 1.A).[13, 14] At pH 7.4, the Aβ peptide is anionic with a charge of about -2.7.

The process by which Aβ peptides self-assemble is very intricate and several species, such as soluble oligomers, amorphous aggregates and proto-fibrils, are formed prior and/or in parallel to the thermodynamically stable and β-sheet rich fibrils.[11, 15, 16] Briefly, the self-assembly proceeds via a nucleation-elongation supramolecular polymerization. It relies on the formation of nuclei that can further elongate at their extremities. In addition, the pool of nuclei can be fueled by secondary nucleation processes, mainly fragmentation and fibril-catalyzed nucleation (Scheme 1.B).[17-23] Association of several fibrils can also occur and lead to twisted fibrils.

View Article Online
DOI: 10.1039/D6QI00446F

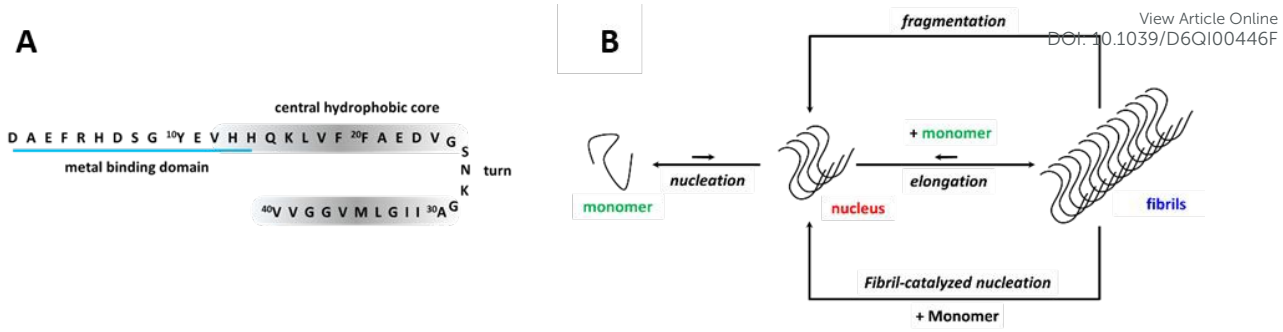

Scheme 1. (A) Sequence of the Aβ(1-40) peptide and regions of interest, (B) Self-assembly process of Aβ peptide.

Inhibition of Aβ self-assembly is considered as a therapeutic approach of interest that can be obtained by employing well-designed molecules,[24-32] beyond immunotherapy.[7-10] Such molecules are aromatic-rich and/or charged compounds able to interact with aromatic, hydrophobic, charged residues and/or metal-binding residues of the Aβ peptide. As a general trend, their mode of action relies on the stabilization of the Aβ peptides under a monomeric form, thus preventing its self-association. Porphyrins have been studied as modulators of the self-assembly of several amyloid-forming peptides. They include Aβ peptide[33-36] but also Tau protein involved in AD,[37] α-synuclein involved in Parkinson's disease,[38-41] insulin,[42, 43] and amylin,[44-46] both being involved in Type-II diabetes.

With respect to Aβ, it has been reported that the stoichiometric ratio of the cationic porphyrin *meso*-5,10,15,20-*tetrakis*(*N*-methylpyridinium-4-yl) porphyrin, **H_2-TMPyP**, inhibits the formation of Aβ(1-42) oligomers and fibrils, induces the dismantling of preformed Aβ aggregates and alleviates Aβ(1-42)-induced cytotoxicity on neuroblastoma SH-SY5Y cells.[33] A neutral porphyrin were very recently reported to have a moderate effect on Aβ self-assembly.[47] Finally, the anionic porphyrin, *meso*-5,10,15,20-*tetrakis*(4-sulfonatophenyl)porphyrin, **H_2-TPPS**, does not influence Aβ(1-42) aggregation[34] while it has some impact on the cationic amylin peptide.[45]

The most typical and characterized example of a metalloporphyrin interacting with Aβ peptide is heme (iron(III)-protoporphyrin IX), which has been found to co-localize with Aβ in senile plaques in post-mortem AD brains and thus attracted much attention. Heme was early shown to modulate Aβ aggregation.[35, 36, 48] The best characterized interaction of heme with Aβ peptides is its coordination with the His residues in a way reminiscent of the heme binding in peroxidase enzymes.[48-51] Zn-porphyrins that can also interact with Aβ His residues have been shown to impact Aβ aggregation as well.[52, 53]

In the present work, we aim at enlarging the family of porphyrins able to interact with Aβ and modulate its self-assembly propensity. Our goal is to release a structure-activity relationship (SAR) and provide deeper insights into their modes of action. Hence, we have studied the effects of a series of cationic porphyrins on the kinetics of Aβ(1-40) self-assembly and on the morphology of the formed

View Article Online
DOI: 10.1039/D6QI00446F

fibrils using a combination of spectroscopic and microscopic imaging methods. We used Aβ(1-40) since it exhibits a more moderate and reproducible self-assembly trends than Aβ(1-42).[54, 55] The porphyrin series includes the commercially available **H_2-TMPyP** and the still unexplored **H_2-MA,** another cationic porphyrin with longer arms. One negatively charged porphyrin (**H_2-TPPS**) is used for comparison purpose. We have also studied the influence of the insertion of two metal cations (Au(III) and Cu(II)) in the center of the cationic porphyrins. In addition, we have probed the effect of porphyrin concentration (*id est*, porphyrin/Aβ(1-40) ratio), a parameter that has not been explored so far. Our data indicate that the TMPyP family interact with Aβ(1-40) peptide leading to an acceleration of the peptide self-assembly and that the MA family induce a biphasic effect. In the latter case, the acceleration is maximal for a given porphyrin concentration that is dependent on the exact nature of the porphyrin. For all the cationic porphyrins studied, the prevention of fibrils formation is observed and increased with the porphyrins' concentration. The deduced SAR shows that (i) interactions between porphyrins and the Aβ peptide are mainly electrostatic and π-stacking forces, while the size of porphyrin also matters; (ii) two sites of interaction co-exist and (iii) the stronger the interactions of the porphyrins with the first site are, the higher the increase of the self-assembly rate is.

Experimental Section

Chemicals and reagents

All the solutions were prepared in ultrapure water. HEPES buffer (2- [4- (2- hydroxyethyl)piperazin- 1- yl]ethanesulfonic acid sodium salt) and ethylenediaminetetraacetic acid (EDTA) were bought from Sigma-Aldrich. ThioflavinT (ThT) was bought from Acros Organics. Anionic porphyrin *meso*-tetra(4-sulfonatophenyl)porphyrin dihydrochloride (**H_2-TPPS**) was purchased from Frontier Scientific. Cationic porphyrins were prepared as previously reported (**H_2-TMPyP** and **H_2-MA**,[56] **Au-MA**[57] and **Cu-MA**[58]). Stock solutions of porphyrins (1 mM) and ThT (250 µM) in water were stored at -20 °C. Aβ(1-40) (sequence DAEFRHDSGYEVHHQKLVFFAEDVGSNKGAIIGLMVGGVV) was purchased from GeneCust (Dudelange, Luxembourg) with a purity grade > 95%. It was purified by FPLC (Fast Protein Liquid Chromatography, size exclusion) according to a previously reported protocol,[59, 60] to obtain a monomeric fraction of Aβ(1-40) prior its use in self-assembly experiments. The peptide concentration was measured by UV-vis absorption of tyrosine (one residue per peptide, Tyr10) at basic pH ($\varepsilon_{293\text{-}360}$ = 2400 M^{-1} cm^{-1}).[61]

View Article Online
DOI: 10.1039/D6QI00446F

Kinetic measurements of Aβ(1-40) self-assembly by ThT and porphyrin fluorescence

Fluorescence experiments were recorded on a FLUOstar OPTIMA BMG LABTECH at 37 °C with black 384-well plate (Greiner BioOne). ThT was excited at 440 nm and the fluorescence emission was recorded at 490 nm. The gain was 1400. Fluorescence was measured at fixed intervals of 10 min preceded by a given period of stirring (15 s at 200 rpm in double orbital mode). The samples were prepared by mixing appropriate volumes of stock solutions of 500 mM HEPES buffer pH 7.4 (containing 100 nM of EDTA), 1 mM porphyrin in water, 250 µM ThT in water and 40 µM Aβ(1-40) peptide in water and about 20% of FPLC eluant (NaCl 150 mM, NaOH 15mM). Final concentrations were: 100 mM HEPES buffer, 20 nM EDTA, 1 to 40 µM porphyrin (see text or figures' captions), 20 µM Aβ(1-40) peptide and 10 µM ThT in a final volume of 50 µL per well. In addition to the measurement of ThT fluorescence during the process of peptide self-assembly, the fluorescence of selected porphyrins was also monitored (excitation at 410 nm and emission at 640 nm, using dedicated filters) every 10 min with a gain value between 1400 and 2700.

Evaluation of kinetic parameters of Aβ assembly.

The ThT fluorescence increase can be considered, in general, as a sigmoidal curve described by the equation: $F(t) = F_0 + \frac{F_{max}-F_0}{1+e^{-k(t-t_{1/2})}} = F_0 + \frac{\Delta F}{1+e^{-k(t-t_{1/2})}}$ where F_0 is the initial ThT fluorescence value, ΔF is the ThT fluorescence increase ($F_{max} - F_0$), k is the growth rate, and $t_{1/2}$ is the time at which the ThT fluorescence increase equals half of its maximal value. To compare all curves, a custom routine was developed to straightforwardly evaluate the key parameters.[60] ThT curves were first normalized. The inflexion point, $t_{1/2}$ was determined as the time at which $F(t) = F_0 + \frac{\Delta F}{2}$. An apparent growth rate, later noted for matter of simplicity $k_{t1/2}$ was estimated by calculating the slope at $t = t_{1/2}$ as $k = 4\left(\frac{F_{60\%}-F_{40\%}}{t_{60\%}-t_{40\%}}\right)$, where $F_{60\%}$ and $F_{40\%}$ equals 60% and 40% of the maximal ThT fluorescence increase, respectively, and $t_{60\%}$ and $t_{40\%}$ are the times at which these fluorescence values occur. The $\frac{1}{4}$ factor arises from the fact that the slope at the inflection point ($t = t_{\frac{1}{2}}$) for a sigmoid equation $S(t) = \frac{1}{1+e^{-k\left(t-t_{\frac{1}{2}}\right)}}$ is equal to $S'(t_{1/2}) = \frac{k}{4}$.

The self-assembly of Aβ(1-40) was studied using several different batches to ensure that the effects seen were not batch-dependent. At least 2 independent experiments with 6 replicates for each condition were performed. Data from one experiment are shown in the full text, other ones can be found in the Supporting Information. To compare the parameters from one experiment to another, normalization with respect to the Aβ(1-40) self-assembly in absence of porphyrins (from the very same

View Article Online
DOI: 10.1039/D6QI00446F

experiment) consisted in dividing the measured mean value of a given parameter by the mean value of the same parameter for the Aβ(1-40) only.

Transmission electron microscopy (TEM).

After 3 days of self-assembly in 384-well plates (see previous paragraph for details), samples were prepared for electron microscopy by using the conventional negative staining procedure. An aliquot (10 µL) of each sample was absorbed on Formvar-carbon coated grids for 1 min, blotted, and negatively stained with uranyl acetate (1%) for 1 min. Grids were examined with a TEM (Jeol JEM-1400, JEOL Inc, Pea- body, MA, USA) at 80 kV. Images were acquired by using a digital camera (Gatan Orius, Gatan Inc, Pleasanton, CA, USA) at different magnifications 3000 (2 µm), 6000 (1 µm), 12000 (0.5 µm scale), and 20000 (100 nm scale).

Atomic force microscopy (AFM)

After 3 days of self-assembly in 384-well plates (see previous paragraph for details), samples were prepared for atomic force microscopy by using a conventional procedure.[62] Briefly, a drop of sample (10 µL) was deposited on a freshly cleaved mica and left for 1 h to adsorb on the substrate. It was then washed with deionized water (50 µL) to remove the salt and dried with pressurized air before imaging. The AFM pictures were taken in air with a Smart SPM-1000 microscope (AISTNT, Novato, USA) equipped with a 100 µM scanner. Si cantilevers (NanoWorld, Swizerland) with an elastic modulus of ≈ 42 $N.m^{-1}$ were used. All images were acquired as 512 x 512-pixel images at a typical scan rate of 0.2 kHz with a vertical tip oscillation frequency of 250-350 kHz. Representative images of each sample were obtained by scanning at least 3 different locations.

UV-visible measurements

Spectra measurements were recorded on an Clariostar fluorimeter in 384 plaques in the very same conditions as ThT experiments at the beginning and the end of the self-assembly process. Porphyrins were put in 100 mM HEPES buffer pH 7.4, 20 nM of EDTA in the absence of peptide or in the presence of 20 µM Aβ(1-40) at 37 °C.

^{1}H-1D-NMR

All spectra were recorded on a Bruker Ascend 600 spectrometer equipped with a 5 mm triple resonance inverse Z-gradient probe (TBI ^{1}H, ^{31}P, BB). Chemical shifts for ^{1}H were relative to TMS (Tetramethylsilane) using ^{1}H (residual) chemical shifts of the solvent as a secondary standard. Peptide concentration was 200 µM in 10 mM HEPES-d_{18} buffer pH 7.4, 10% D_2O. Porphyrins were dissolved in H_2O at 1 mM concentration and appropriate aliquots were added to the test tube so that the final molar ratio varied from 1% to 20% of porphyrin. The ^{1}H-NMR spectra were acquired at 298K using the Bruker pulse program 'zgesp' featuring a water-suppression sequence and the following parameters:

View Article Online
DOI: 10.1039/D6QI00446F

spectral width, 12 ppm; 30° nutation angle duration, 9.5 µs; recycling delay, 2-s (1-s acquisition time and 1-s relaxation delay).

Results and discussion

The porphyrins used in the present study are shown in Scheme 2. They are charged and thus soluble in water. The non-metallated porphyrin scaffold bears four charges, located at different positions on the *meso*-substituents. Our study introduces **H_2-MA**, a novel porphyrin that has not been investigated in the context of amyloid formation. Structurally, **H_2-MA** features four identical arms, and is derived from the commercially available and previously studied **H_2-TMPyP** (Scheme 2.A) and has been originally synthesized for interacting with the minor groove of DNA.[56, 63] **H_2-MA** has been chosen to explore the influence of arm length and aromatic interactions while maintaining the same charge as **H_2-TMPyP**. The extended aromatic system in **H_2-MA** enhances π-stacking interactions and electron delocalization, potentially amplifying its effect on Aβ self-assembly. Its positive charge is farther from the tetrapyrrole scaffold compared to the reference **H_2-TMPyP** since the *meso*-substituents are bulkier than the pyridinium groups of **H_2-TMPyP**. Furthermore, the electron richness of the porphyrin core is higher than that of **H_2-TMPyP** due to the remoteness of the pyridinium groups. Au(III) counterparts of the **H_2-TMPyP** and **H_2-MA** as well as the Cu(II)-**MA** were also included in the study. While Fe-,[36, 38, 39, 45, 46, 64] Zn-,[34, 47, 53] and Mn-porphyrins[34, 46, 64, 65] have been studied in the context of amyloid-forming peptide self-assembly, Cu-[34, 43] and Au- porphyrins have received less attention in the literature. This highlights an opportunity to further exploration of these metalloporphyrin's in modulating Aβ self-assembly.

The commercially available anionic porphyrin, **H_2-TPPS**, bearing four negative charges, was included in the series of the tested compounds for comparison purpose (Scheme 2.B).

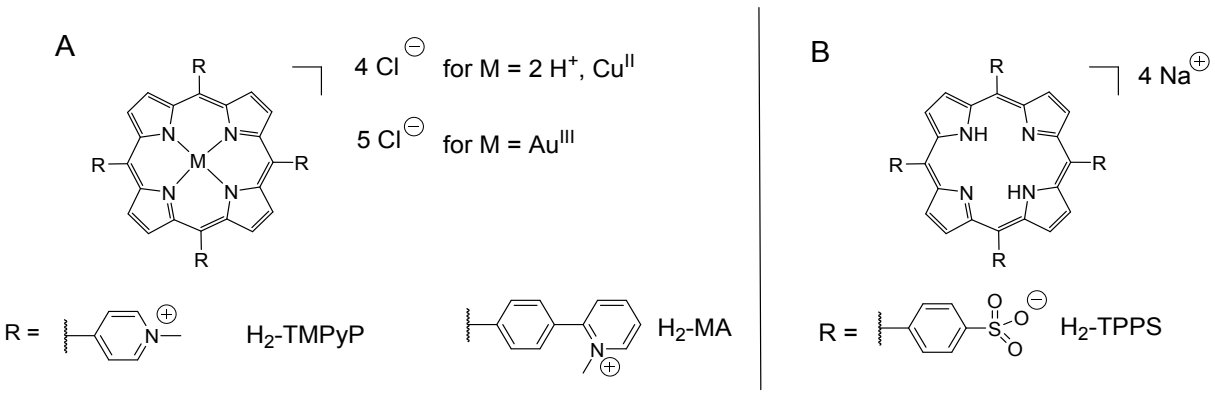

Scheme 2. (A) Structures of the cationic porphyrins, M = 2 H^+ stands for the non-metalled porphyrins and (B) structure of the anionic porphyrin.

View Article Online
DOI: 10.1039/D6QI00446F

1- Influence of the porphyrins on the fibrillation of Aβ(1-40) peptide

The self-assembly of Aβ(1-40) was monitored by a standard approach using thioflavin T (ThT)[66, 67] fluorescence and TEM and AFM imaging at the end of the self-assembly. 2 to 4 independent experiments were performed for each porphyrin (see Table S1 for the numbering of the various experiments and the porphyrins included). The experiments were performed in 384-wells plates at 37 °C, with 20 µM peptide concentration. The concentration of porphyrin varied from 0.1 µM to 40 µM depending on the tested porphyrin. All the ThT fluorescence kinetic curves exhibit a typical sigmoid appearance (Figures 1 and S2), characterized by an initial lag phase corresponding to nucleation, a growth phase linked to elongation and secondary nucleation processes, and a final stationary phase. Three key kinetic parameters describing the self-assembly process will be discussed in the following: the difference between the initial and final fluorescence intensities, ΔF; the time at which the fluorescence intensity has increased of ΔF/2, $t_{1/2}$; and the slope at $t_{1/2}$, $k_{t1/2}$. Comparison of the influence of porphyrins on these kinetic parameters is shown in Figure 2 (see Figures S3-S5 for the additional self-assembly experiments). The obtained results highlight the good reproducibility of the trends observed between independent experiments. Besides, TEM and AFM images of the formed assemblies recorded at the end of the fluorescence experiments give insights on their morphology and size. They are are shown in Figure 1 and Figures S6-S7 for the additional self-assembly experiments

First, the negatively-charged porphyrin **H_2-TPPS** was tested at various concentrations (from 2 µM to 40 µM). Self-assembly parameters are virtually identical (Figure 1.A and Figure 2), except for the maximum of ThT fluorescence intensity for which a slight decrease is observed. TEM images indicate that the twisted structure build on 3-4 fibrils is conserved even at 10 µM concentration in porphyrin (compare Figure 1.E and S6.B with Figure 1.D and S6.A). Hence, **H_2-TPPS** neither affect the kinetics of Aβ(1-40) self-assembly nor change the structure of the fibrils, indicating that it does not modify significantly Aβ(1-40) peptide self-assembly in line with reported data on Aβ(1-42).[34]

View Article Online
DOI: 10.1039/D6QI00446F

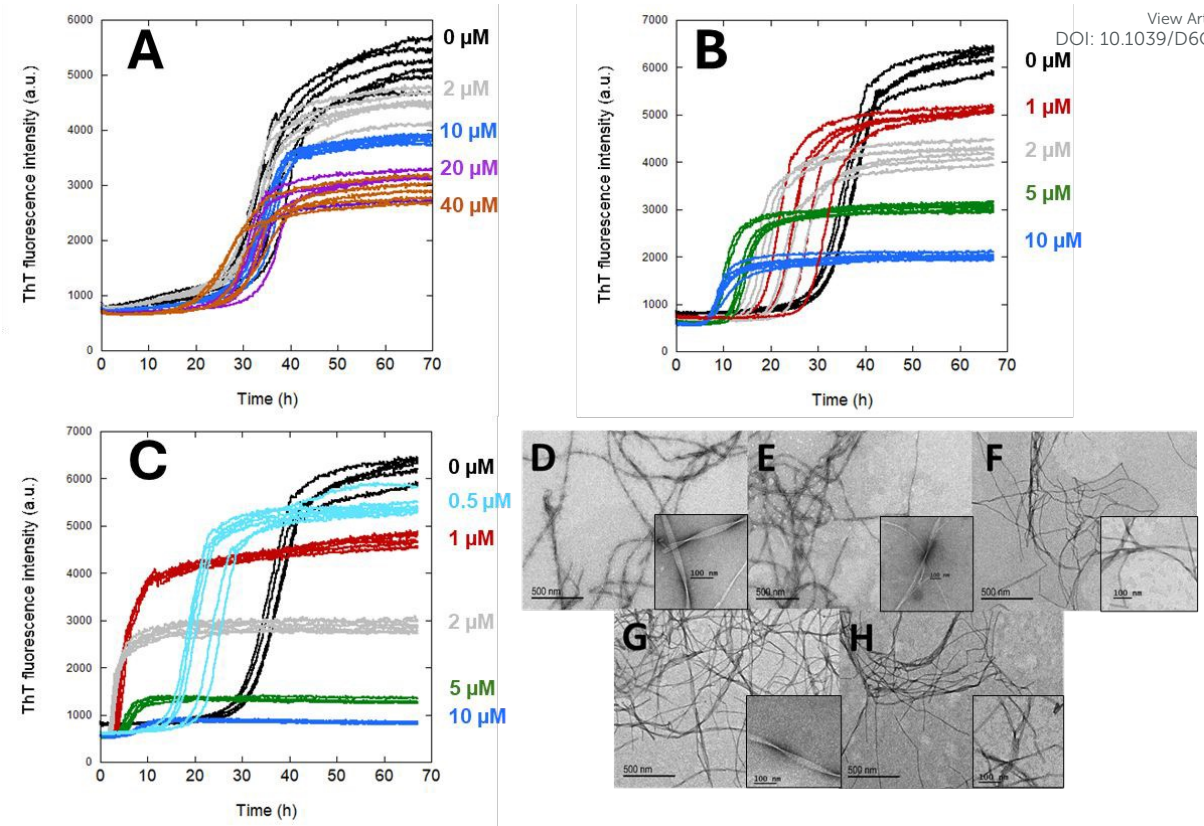

Figure 1. Self-assembly of Aβ(1-40) peptide (20 µM) in the presence of various concentrations of porphyrins in 100 mM HEPES buffer pH 7.4, at 37 °C. ThT fluorescence kinetic curves in presence of (A) **H_2-TPPS** (from experiment N°2), (B) **H_2-TMPyP** and (C) **H_2-MA** (from experiment N°1). Black: Aβ(1-40) peptide, light blue, red, grey, green, dark blue, violet and brown in presence of 0.5, 1, 2, 5, 10, 20 and 40 µM of porphyrin, respectively. Six replicates are shown to illustrate the reproducibility. Corresponding TEM images, at two different magnifications, of the fibrils morphologies obtained after 3 days: (D) 20 µM Aβ(1-40) and in the presence of (E) 10 µM **H_2-TPPS**, (F) 1 µM **H_2-TMPyP**, (G) 10 µM **H_2-TMPyP**, (H) 1 µM **H_2-MA**.

In contrast to what was observed in the presence of **H_2-TPPS**, significant changes are observed on the Aβ(1-40) self-assembly curves in the presence of cationic porphyrins (Figure 1.B, 1.C and S2). Their addition leads to a significant acceleration of the Aβ(1-40) self-assembly that depends on the porphyrin nature and concentration as reflected by the corresponding decrease of the $t_{1/2}$ (Figure 2.A and Figures S4.A-S5.A). In the case of **H_2-TMPyP**, the $t_{1/2}$ decreases with a monotonic concentration-dependence with a maximal acceleration effect observed at the highest tested concentration (Figures 2.A and Figure S4.A). In the case of **H_2-MA**, the $t_{1/2}$ decreases until the porphyrin concentration reaches a concentration of 2 µM and re-increases at higher concentrations (Figure 2.A and Figure S5.A). The concentration corresponding to the maximal acceleration is noted C_M. The accelerating effect of both porphyrins can be compared at 1 µM. The Aβ(1-40) self-assembly was extremely rapid in presence of **H_2-MA**, the $t_{1/2}$ being 10 times shorter than that of the control (normalized $t_{1/2}$ = 0.1, Figure 2.A and S5.A), in contrast to **H_2-TMPyP** with a normalized $t_{1/2}$ = 0.7 (Figure 2.A and S4.A). Similar porphyrin-dependent trends are observed for the slope $k_{t1/2}$ of the growth phase. Indeed, **H_2-TMPyP** induced a weak and monotonic increase of the $k_{t1/2}$ and **H_2-MA** a much steeper increase, maximal at 2 µM, Figures 2.B and S4-5.B. A monotonic versus a biphasic variation are thus detected on both the $t_{1/2}$ and $k_{t1/2}$

View Article Online
DOI: 10.1039/D6QI00446F

upon addition of **H_2-TMPyP** and **H_2-MA**, respectively. This indicates that the porphyrin's nature and concentration-dependent effect not only concern the nucleation step but also the growth phase of the Aβ(1-40) self-assembly.

Besides, as shown in Figure 1 and 2.C (and Figures S4-5.C), a decrease of the maximum fluorescence intensity (F_{max}) with the increase of the porphyrins' concentration is observed. It can have several origins: (i) the porphyrins absorb at λ = 440 nm at which ThT is excited. Hence, they can induce a significant inner-filter effect (IFE, that limits the level of absorbed light to excite ThT). The extent of the IFE is dependent on the molar extinction coefficient (ε) of each porphyrin (see Table S2) and of their concentration. IFE follows the equation $10^{-(abs*[porph])}$ where abs is a constant value that combine the ε value and the pathlength. For a given porphyrin, the decrease observed in the ThT fluorescence doesn't correspond to this law. In addition, the ThT fluorescence decrease doesn't correspond to the respective ε values of the added porphyrins. More precisely, the effect observed is **H_2-MA** > **H_2-TMPyP** > **H_2-TPPS** although the ε value (**H_2-TMPyP** > **H_2-MA** > **H_2-TPPS**). In addition, porphyrins undergo a hypochromic effect during interaction with Aβ(1-40) and Aβ(1-40) self-assembly (Figure 3, vide infra) which is stronger for H_2-MA versus the other two porphyrins. Altogether, this indicates that IFE is not predominant in the case of **H_2-MA**; (ii) the porphyrins induce the decrease of the number of fibrils formed and/or a change in their morphology, with the formation of Aβ(1-40) fibrils less responsive to ThT; (iii) the porphyrins and ThT compete for the same binding site into the fibrils. It is likely that the three effects occur. The extent to which they contribute to the observed decrease of the ThT fluorescence is extremely difficult to assess quantitatively. Hence to evaluate the effect of cationic porphyrins on the formation of Aβ(1-40) fibrils, both on the level of fibrils formation and/or the morphology, the Aβ(1-40) self-assembly media were recovered after four days at 37 °C and were analyzed by microscopic imaging (TEM and AFM). The TEM image of the Aβ(1-40) control shows the classic long twisted assembly based on 3-4 fibrils of Aβ (Figure 1.D and Figure S6.A).[68] In the presence of **H_2-TMPyP** at 1 µM and 10 µM (Figure 1.E,F and Figure S6.C, respectively), and **H_2-MA** 1 µM (Figure 1.H and S6.E) thinner assemblies (some of them build on 2 fibrils) are observed with no clear differences between images. In the media containing 10 µM **H_2-MA** no fibrils were found neither on the TEM grids (not shown) nor on the AFM chips although they were searched with the greatest care. AFM was also performed at the intermediate concentration of 5 µM to grasp some species with lower molecular weights for **H_2-TMPyP** or **H_2-MA** and the obtained pictures show the presence of numerous fibrils in presence of **H_2-TMPyP** whereas very few fibrils were observed for **H_2-MA** (Figure S7)**.**

In summary, the cationic porphyrins are able to influence Aβ(1-40) self-assembly by changing its rate and by preventing the formation of fibrils in a concentration-dependent manner. We observe two effects. For **H_2-TMPyP**, a monotonic acceleration of the Aβ(1-40) self-assembly is observed

View Article Online
DOI: 10.1039/D6QI00446F

(decrease in $t_{1/2}$, Figures 2.A and S4.A) and the morphology of the fibrils is altered as thinner fibrils are detected by TEM at 1 and 10 µM (Figure 1.F, 1.G, S6.C and S6.D). For **H_2-MA**, the kinetic effect follows a bell-shape curve (Figures 2.A and S5.A), with a maximal acceleration of the Aβ(1-40) self-assembly observed at C_M ~ 2 µM. Thinner fibrils were observed by TEM at 1 µM (Figure 1.H and Figure S6.E) and no fibrils were observed at 10 µM.

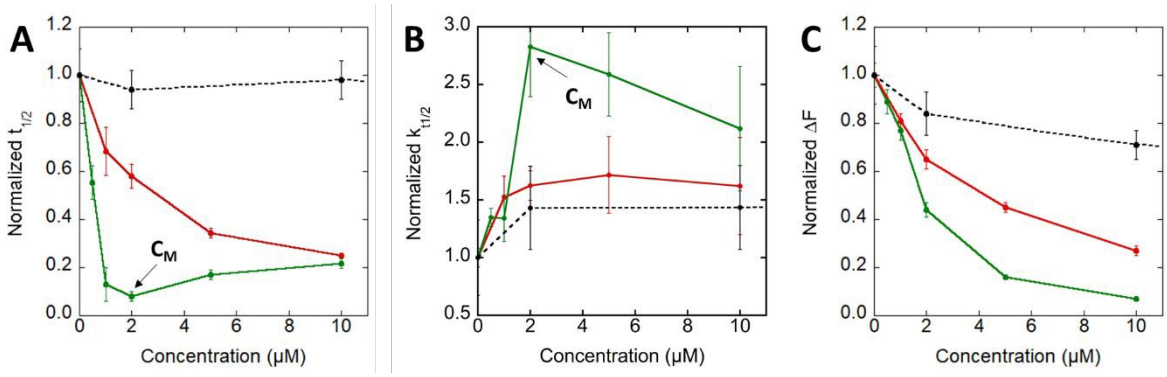

Figure 2. Kinetic parameters describing the concentration-dependent effect of porphyrins on Aβ(1-40) self-assembly. (A) Normalized $t_{1/2}$; (B) Normalized $k_{t1/2}$ and (C) Normalized ΔF (Normalization is based on the parameters of the peptide alone, see Experimental Section for details). Red **H_2-TMPyP**, green **H_2-MA**, and black **H_2-TPPS.** C_M corresponds to the concentration where the accelerating effect of the porphyrins is maximum. Data from Figure 1.

2- Interactions of non-metallated porphyrins with monomeric and self-assembled Aβ(1-40)

UV-vis spectroscopy

To probe the interaction between the porphyrin and Aβ, UV-vis absorption spectra of porphyrins were recorded in absence or presence of monomeric and self-assembled Aβ(1-40) (Figure 3). The spectra of all the porphyrins don't change in the presence of the monomeric Aβ(1-40).

The UV-vis spectra of the anionic porphyrin, **H_2-TPPS**, did not significantly change during the self-assembly of Aβ(1-40) (λ_{max} = 415 nm) (Figure 3.A). In contrast, the spectra recorded at the end of Aβ(1-40) self-assembly in presence of 2 µM of the other porphyrins show a shifted Soret absorbance peak for **H_2-TMPyP**, from 423 to 432 nm ($\Delta\lambda$ = 9 nm) (Figure 3.B) and for **H_2-MA**, from 418 to 424 nm ($\Delta\lambda$ = 6 nm) (Figure 3.C). These bathochromic shifts together with the associated hypochromic effect is a typical signature of the porphyrin macrocycle undergoing π-stacking interactions with its environment.[69, 70]

View Article Online
DOI: 10.1039/D6QI00446F

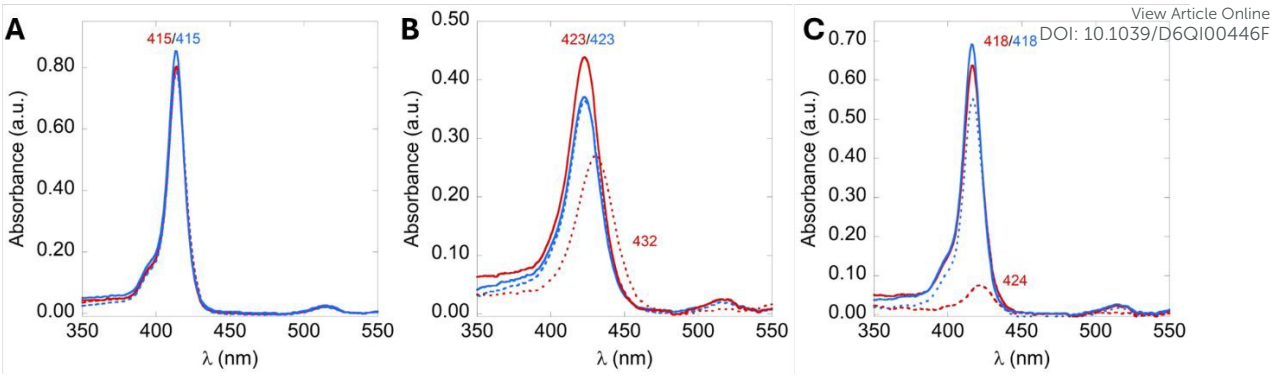

Figure 3. UV-visible spectra of 2 µM porphyrin with (red) or without Aβ(1-40) (blue), before (plain lines) and at the end of the Aβ(1-40) self-assembly (dotted lines). (A) **H_2-TPPS**, (B) **H_2-TMPyP**, (C) **H_2-MA**,). [Aβ(1-40)] = 20 µM, [hepes] = 100mM, pH 7.4, T= 37 °C and ℓ = 1 cm.

Fluorescence

We then take advantage of the intrinsic fluorescence of non-metallated porphyrins[71-73] to kinetically monitor Aβ(1-40) self-assembly. The changes induced by the peptide self-assembly on the fluorescence was followed at λ_{ex} = 410 nm and λ_{em} = 640 nm (Figures 4.A, S8-S9). The fluorescence of the porphyrin decreases along a sigmoidal curve reminiscent of what is observed for ThT. However a shorter $t_{1/2}$ is measured, indicating that the events probed precede the formation of the well-organized β-sheet-rich fibrils detected by ThT fluorescence (Figures 4.A, S8-S9). The difference between the two characteristic times is noted $\Delta t_{1/2}$ (Figure 4.A). The extent of the decrease in porphyrin fluorescence is about 15% for **H_2-TMPyP** and 65% for **H_2-MA** while the $\Delta t_{1/2}$ is about 0.3 h for **H_2-MA** and null for **H_2-TMPyP** (Figures 4.B and S8-9, Table S3) at 5 µM. This may witness the extent of the hydrophobic interaction between the porphyrins and the species formed prior Aβ(1-40) fibrils (later noted nuclei). For **H_2-MA**, but not **H_2-TMPyP** that has a too weak fluorescence (Figure S8.A), a concentration–dependent study (between 1 to 10 µM) was also performed (Figure S9 and Table S4). Two trends can be observed: (i) the decrease in the porphyrin fluorescence intensity is virtually independent of the porphyrin concentration (Table S4) and (ii) the $\Delta t_{1/2}$ decreases when the porphyrin concentration increases (Figure 4.B). This indicates that the various equilibria at play in the Aβ(1-40) self-assembly are differently altered by the porphyrin concentration, with higher concentrations of porphyrin favoring higher molecular weight species. In brief, the gradual change in the fluorescence of the porphyrins during fibrillation indicates that they interact with the peptide under a specific environment that is not yet Aβ(1-40) fibrils. The decrease of porphyrin fluorescence may be linked to interaction with Aβ(1-40) intermediate-size assemblies able to provide an hydrophobic environment as those encountered during intercalation between DNA base pairs.[70]

View Article Online
DOI: 10.1039/D6QI00446F

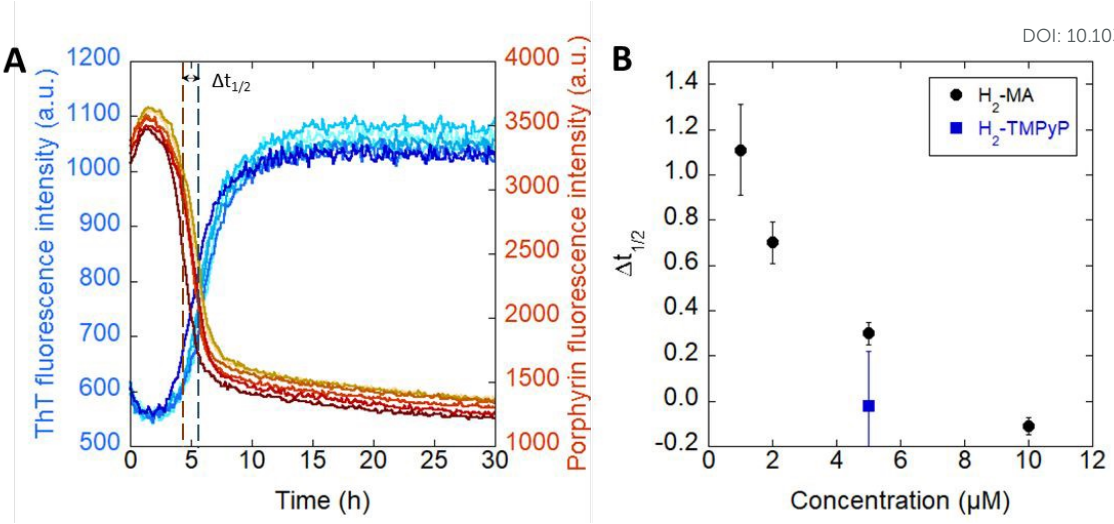

Figure 4. A) Kinetic curves of Aβ(1-40) self-assembly (20 μM) in the presence of **H_2-MA** (black circles in panel B) at 5 μM recorded at λ_{em} = 640 (excitation at λ=410 nm). Brownish lines correspond to the fluorescence of the porphyrin versus that of ThT in blue lines. Lines are replicates from one experiment and B) Difference between the $t_{1/2}$ detected by the fluorescence of porphyrin (brownish dotted line in Panel A) and ThT (blue dotted line in Panel A) as function of porphyrin concentration. Black circles: **H_2-MA** at different concentrations and blue square: **H_2-TMPyP** at 5 μM.

NMR

The NMR spectra of Aβ(1-40) were recorded in the presence of 0.1 equiv. of **H_2-TPPS**, **H_2-TMPyP** and **H_2-MA** (Figure 5, see Figures S10-13 for other spectral domains and stoichiometry). Attribution of key residues were performed according to literature.[74-78] In the 7.50 – 7.70 ppm region five singlets corresponding to the three Hε protons of His6, His13 and His14 and to two amide NH protons (the first one is from Val40 NH, the second one is not attributed) are detected. The signals between 6.95 and 7.25 ppm are attributed to Phe4, Phe19 and Phe20 residues. Tyr10 aromatic protons appear as two doublets at δ = 6.65 and 6.92 ppm. Finally, three singlets at δ = 6.77, 6.78 and 6.86 ppm corresponding to the three Hδ of His6, His13 and His14 of Aβ(1-40), in addition to two non-attributed amide NH protons, are detected. Upon addition of porphyrins, a shift of all aromatic peaks is observed that is linked to π-stacking interaction between the tetrapyrrolic ring of the porphyrin and the aromatic residues. A stronger shift is detected for the **H_2-MA** > **H_2-TMPyP** > **H_2-TPPS** thus mirroring a stronger interaction between **H_2-MA** and the peptide. Similar trends are observed on the Hβ (Figure S11), and on the -Me group of Met35 (Figure S12), Val12 and Val18 (Figure S13). This indicates a preferential binding of the porphyrins to the hydrophobic core of the peptide (Scheme 1.A). For the three porphyrins, the aromatic His peaks are less shifted than the Phe and Tyr ones. This may be linked to the partly protonated state of the His at pH 7.4 disfavoring the interaction with the cationic porphyrins. NMR confirms the trend previously observed by UV-vis and fluorescence with respect to the strength of the interaction between the porphyrins and the Aβ(1-40).

View Article Online
DOI: 10.1039/D6QI00446F

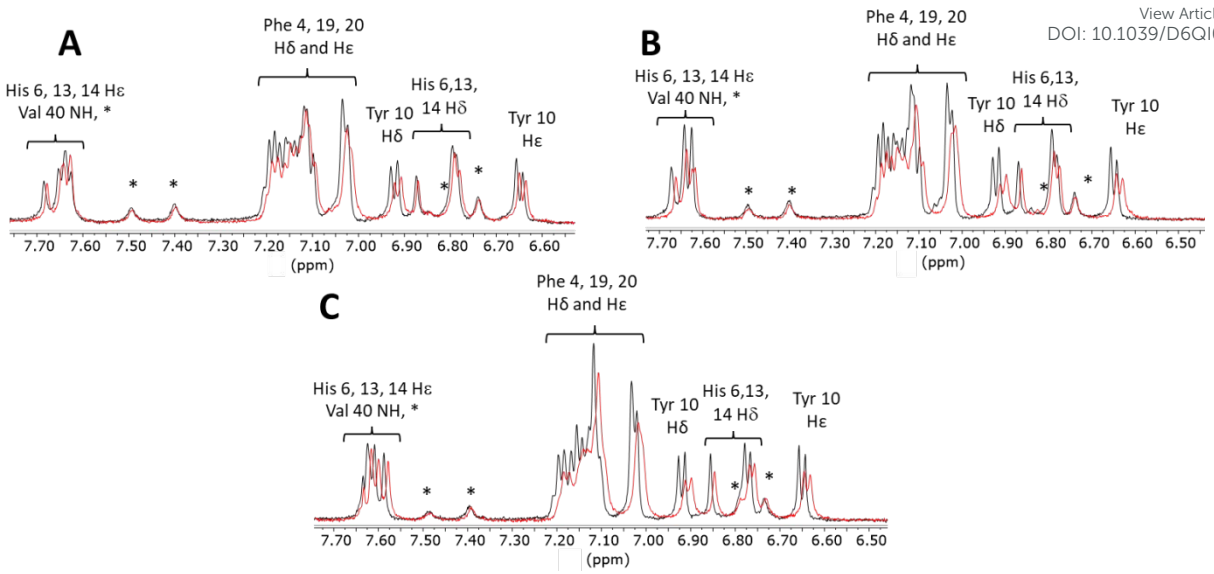

Figure 5. ^{1}H-NMR spectra of selected aromatic regions of Aβ(1-40) 200 µM, pH 7.4 in 10 mM of d^{18}-HEPES buffer (10% D_2O). control (black trace) and in the presence of 0.1 equiv. (red trace) of added porphyrin (A) **H_2-TPPS**, (B) **H_2-TMPyP** and (C) **H_2-MA**. Signals marked * stand for non-attributed NH amide protons.

3- Influence of the metallated porphyrins on the fibrillation of Aβ(1-40) peptide

To go further and aiming at having other probes of the interaction with Aβ(1-40), we used Cu(II) and Au(III) derivatives of the cationic porphyrins. Such metalation keeps the flat shape of the porphyrin as no apical ligation occurs,[79, 80] but changes the charge (in the case of Au(III)) and lowers the electron density of the ligand aromatic system thus increasing the π-stacking properties.[81, 82]

The effect of pentacationic **Au(III)-MA**, **Au(III)-TMPyP**, and tetracationic **Cu(II)-MA** porphyrins (Scheme 2) was tested on the self-assembly of Aβ(1-40) (Figure S14). In the case of **Au-TMPyP**, the monotonic accelerating effect is stronger than the one detected for the **H_2-TMPyP** (Figure S15.A). In the case of **Au-MA**, a concentration-dependence similar to that of **H_2-MA** is observed (Figures 6.A-B and S2.C-D) where the threshold value (C_M) is obtained for a lower porphyrin concentration (1 µM for **Au-MA** versus 2 µM for **H_2-MA** (Figures 7.A and S17.A). In the case of **Cu-MA** (Figure 6.C and S2.E), effects similar to **H_2-MA** are observed. For the three metalated porphyrins, the evolution of the maximal ThT fluorescence values is similar than for the apo-counterpart (Figures 7.C and S17-S18.C). Among the three possible origins of the observed ThT fluorescence decrease, as described previously, the inner-filter effect may not contribute significantly as the molar extinction coefficient values of the metalated porphyrins are weaker than the free base porphyrins (Figure S16 and Table S2).

TEM pictures were taken after the self-assembly of Aβ(1-40) in presence of 1 µM of metallated porphyrin (Figure 6.F-G and S7.F-G). All the porphyrins do induce a change in Aβ(1-40) fibrils morphology but to a different extent: **Cu-MA** has the same effect as **H_2-MA** (compare Figure 6.G with Figure 6.E), the fibrils formed in presence of **Au-MA** are longer and larger and exhibit well-resolved

View Article Online
DOI: 10.1039/D6QI00446F

twists and nodes, although they were less numerous (Figure 6.F). At 10 µM of metallated porphyrins, no fibrils were detected on the TEM grids. AFM was performed at 5 µM and spherical and toroidal objects of about 20-40 nm and 30-100 nm were detected for **Cu-MA** and **Au-MA**, respectively (Figure S19). Hence, the TEM and AFM imaging indicate that the diminution of ThT fluorescence in case of **Cu-MA** and **Au-MA** is mainly linked to the formation of non-fibrillar species.

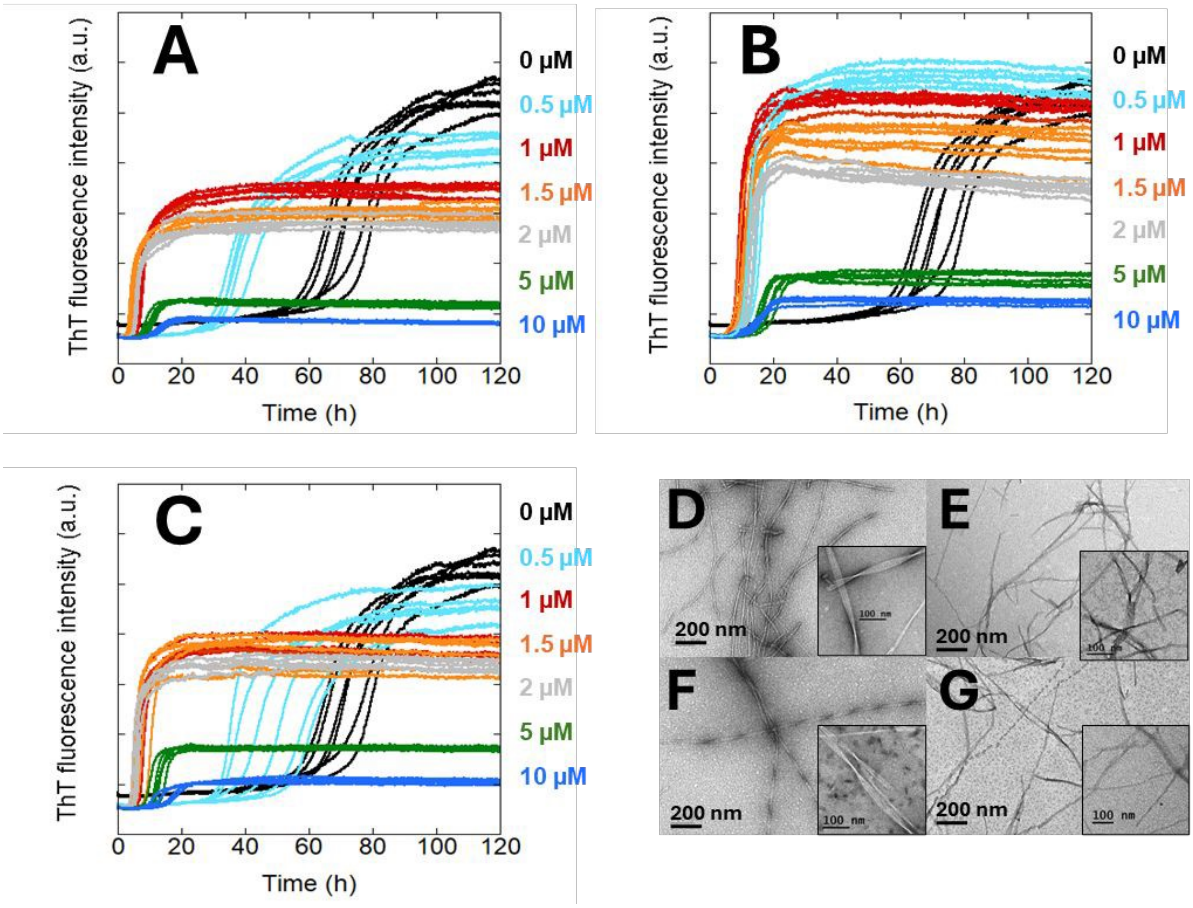

Figure 6. Self-assembly of Aβ(1-40) peptide (20 µM) in the presence of various concentrations of porphyrins in 100 mM HEPES buffer pH 7.4, at 37 °C. ThT fluorescence kinetic curves in presence of (A) **H_2-MA** (from experiment N°3), (B) **Au-MA** (from experiment N°3) and (C) **Cu-MA** (from experiment N°3). Black: Aβ(1-40) peptide, light blue, red, orange, grey, green and blue in presence of 0.5, 1, 1.5, 2, 5, 10 µM of porphyrin, respectively. Note that the fluorescence intensity has the same scale for all the graphs. Six replicates are shown to illustrate the reproducibility. Corresponding TEM images, at two magnifications, of the fibrils morphologies obtained after 3 days: (D) 20 µM Aβ(1-40) and in the presence of (E) 10 µM **H_2-MA**, (F) 1 µM **Au-MA**, (G) 1 µM **Cu-MA**.

View Article Online
DOI: 10.1039/D6QI00446F

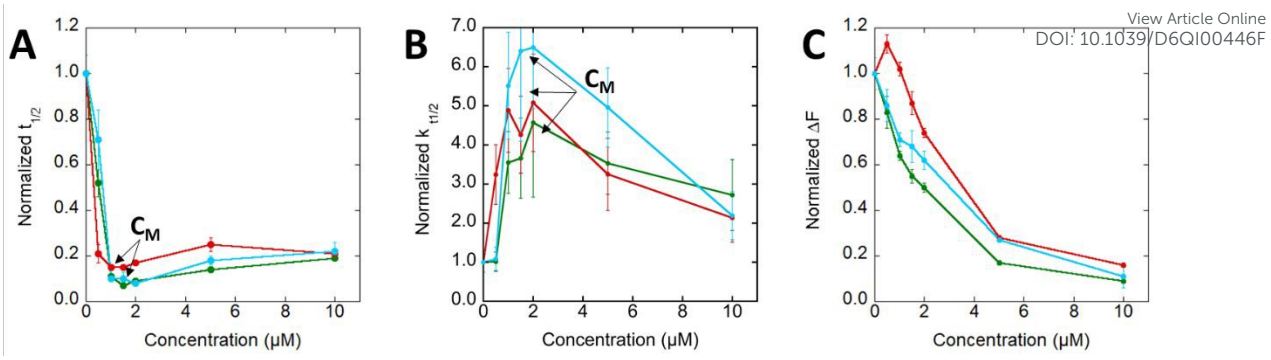

Figure 7. Kinetic parameters describing the concentration-dependent effect of porphyrins on Aβ(1-40) self-assembly. (A) Normalized $t_{1/2}$; (B) Normalized $k_{t1/2}$ and (C) Normalized ΔF (Normalization is based on the parameters of the peptide alone, see Experimental Section for details). Red **Au-MA**, green **H_2-MA**, and blue **Cu-MA.** C_M corresponds to the concentration where the accelerating effect of the porphyrins is maximum. Data from Figure 6.

In brief, the **Cu(II)-MA** porphyrin has a similar effect on Aβ(1-40) self-assembly than the **H_2-MA**. This is in line with the two compounds having the same number of charges. In contrast, the **Au(III)-MA** increased the capacity of the porphyrin to change the kinetics of Aβ(1-40) self-assembly compared to the non-metallated counterpart. This is due to an extra positive charge and a stronger π-stacking capacity, both properties being anticipated to enhance the interaction with Aβ(1-40).

4- Interactions of metallated porphyrins with the monomeric and self-assembled Aβ(1-40)

The interactions of the metalated porphyrin were then probed by UV-vis and by ^{1}H NMR (Figure 8) with the aim to relate them to the impact of the porphyrins on Aβ(1-40) self-assembly. In UV-vis, the trend observed is a bathochromic shift where **Au-MA** > **Cu-MA** ~ **H_2-MA**, in line with the effect observed on Aβ(1-40) self-assembly. In NMR, the modifications induced on the peptide spectrum depends on the porphyrin at play. In case of the diamagnetic **Au-MA** (Figure 8.E), shift of key residues' peaks reminiscent to what was observed previously for **H_2-MA** is detected but to a greater extent (Figure 8.D). Indeed, 10 % of **Au-MA** induces a higher shielding ($\Delta\delta \sim 0.06 - 0.1$ ppm) of Phe and Tyr aromatic protons and also a stronger broadening keeping the His residues weakly affected (Figure 8.E). In the aliphatic region, the induced shift of specific peaks (Hβ of Phe20, His6, His13, His14, Tyr10, Ala (Figures S21, 22.A & B), Hγ of Val12 & 18, (Figure S23.A & B) is also stronger for **Au-MA** versus **H_2-MA**. The addition of the paramagnetic **Cu-MA** porphyrin leads to broadening effects rather than shifts for the diamagnetic porphyrins previously described.[83] When added at 2% molar ratio (Figure 8.F), the protons (Hδ, Hε) of the His were not significantly affected, yet the intensity of the Tyr (Hε, Hδ) protons decreased. With 10% of **Cu-MA**, the signals of the Phe aromatic residues broadened, the Tyr signals vanished with the His signals remaining less affected (Figure S20.C). Given the fact that Cu(II) doesn't bind the Tyr of the Aβ peptide,[84] it is unlikely that Cu(II) inside a porphyrin scaffold does. Hence, the interactions are mainly π-stacking /hydrophobic. For the three Phe residues (Phe4, Phe19, Phe20), as their signals superimpose, it is difficult to identify whether one or two are most affected

View Article Online
DOI: 10.1039/D6QI00446F

than the other(s). In the aliphatic region, strong broadening is also observed on Hβ of His and Tyr (Figure S21.C), of Leu17/34 and Hγ of Val 12 and 18, and the Me group of Met (Figures S22.C and S23.C). For the three porphyrins, the same residues are affected, mostly lying in the CHC. **Au-MA** had a greater effect than **H_2-MA** in line with a stronger interaction by π-stacking and the higher modulation of the Aβ(1-40) self-assembly.

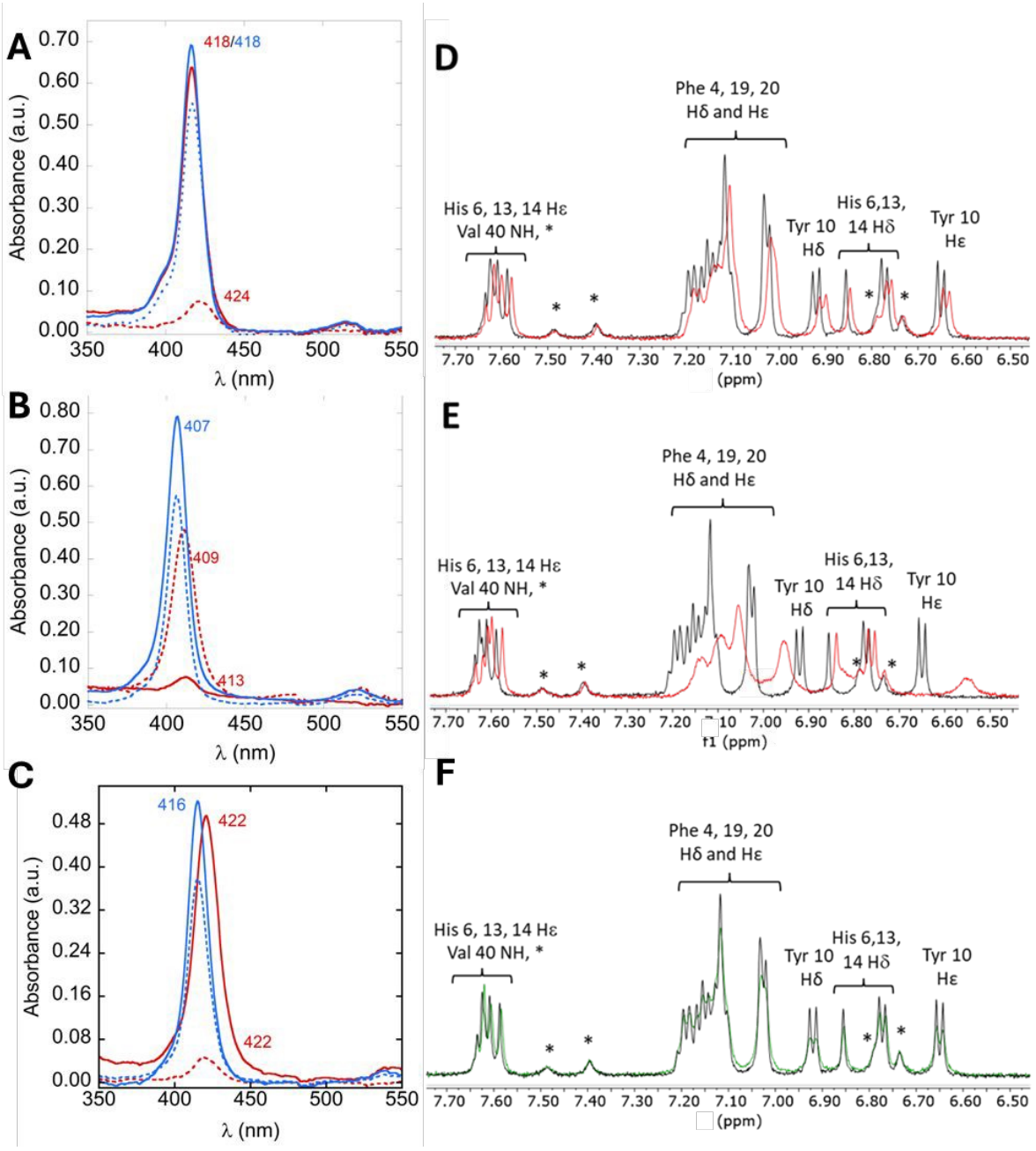

Figure 8. UV-visible spectra of 2 µM porphyrin with (red) or without Aβ(1-40) (blue), before (plain lines) and at the end of the Aβ(1-40) self-assembly (dotted lines). (A) **H_2-MA**, (B) **Au-MA**, (C) **Cu-MA**. [Aβ(1-40)] = 20 µM, [Hepes] = 100mM, pH 7.4, T= 37 °C and ℓ = 1 cm. ^{1}H-NMR spectra of selected aromatic regions of Aβ(1-40) 200 µM, pH 7.4 in 10 mM of d^{18}-HEPES buffer (10% D_2O). control (black trace) and in the presence of 0.02 equiv. (green trace) or 0.1 equiv. (red trace) of added porphyrin (D) **H_2-MA**, (E) **Au-TMPyP** and (F) **Cu-MA**. Signals marked * stand for non-attributed NH amide protons.

View Article Online
DOI: 10.1039/D6QI00446F

5- Possible mechanism(s) at play

In the present study that has scrutinized the effects of a family of porphyrins on the Aβ(1-40) self-assembly, as well as the interactions between the porphyrins and the peptide, several trends were observed that are reminded and discussed below.

(1) The effect of the porphyrins on the Aβ(1-40) self-assembly depends on the chemical nature of the porphyrins, which can be gathered into three families. The anionic **H_2-TPPS** porphyrin has virtually no impact on Aβ(1-40) self-assembly. The **H_2-TMPyP** and **Au-TMPyP** exert an accelerating effect that monotonically increases with the porphyrin concentration (up to the concentration values studied). Finally, the **H_2-MA**, Cu-MA and Au-MA that induce a biphasic trend, for which the accelerating effect reaches a maximum at a given concentration (C_M that generally lies in the 1-2 µM range or, otherwise stated, 0.05-0.1 equiv. per Aβ(1-40) peptide). We propose that the three types of effects observed (no effect, monotonic and biphasic fastening of the assembly) are linked to the strength of the interactions of the porphyrins with the Aβ(1-40) peptide, either in its monomeric form as probed by NMR and UV-Vis (Figures 3, 5 and 8) or once self-assembled as probed by fluorescence and UV-Vis (Figures 3, 6 and 8).

(2) The anionic porphyrin weakly interacts with the Aβ(1-40) peptide that is globally negatively charged at neutral pH (overall charge = -2.7) and that possesses a unique cationic residue (Lys16) at the edge of the CHC versus two anionic residues in the middle of the CHC (Scheme 1.B). The cationic porphyrins have effects that depend on the length of the cationic arms, with **H_2-MA** exhibiting stronger effects than **H_2-TMPyP** on Aβ(1-40) self-assembly (Figures 1-2).

(3) Cu-MA porphyrin shows similar accelerating effect of Aβ(1-40) self-assembly than the parent **H_2-MA**; a stronger effect is observed for **Au-MA** in line with a higher hydrophobicity of the aromatic ring and higher number of positive charges.

We propose that the cationic porphyrins interact in the CHC of the Aβ(1-40) peptide and that two main forces are important:

(i) the hydrophobicity (**H_2-TMPyP** < **H_2-MA** ~ **Cu-MA** < **Au-MA**) and the resulting stacking interactions with the aromatic residues (Phe 19 & 20) and hydrophobic interactions with Val12 and Val18, and Leu17 as probed by NMR (Figures 5, 8, S10-13 and S20-23);

(ii) the electrostatic interactions with anionic residues (mainly Glu22, Asp23) that is expected to increase with the accessibility of the porphyrin cationic arms (**H_2-TMPyP** < **H_2-MA)**. The stronger these interactions are, the stronger the effects on the kinetics of Aβ(1-40) self-assembly and on the prevention of fibrils formation (Figures 1, 6, S6, S7 and S19).

View Article Online
DOI: 10.1039/D6QI00446F

Scheme 3 summarizes the proposed main site of interactions of each porphyrin with the Aβ(1-40) peptides; the possible second site of interactions is shown in Scheme S1. We used the rough diameter of the porphyrin to estimate the porphyrin / peptide ratio.[33] According to a very simplified estimation, about 4 and 5 peptides should be required to host **H_2-TMPyP** and **H_2-MA,** respectively.

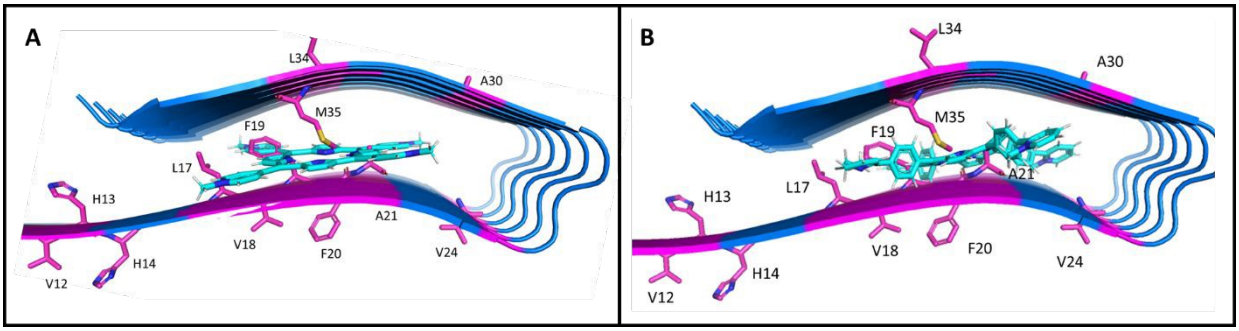

Scheme 3. Representation of the interactions of the porphyrin with Aβ(1-40) peptide. A) **H_2-TMPyP**, B) **MA** family. Drawings based on 5 Aβ(1-40) using alphafold3).[85] Interacting amino acids are shown in pink.

Further, to explain the changes induced by the porphyrins on the Aβ(1-40) self-assembly, we propose a simplified mechanism shown in Scheme 4 for the **MA** family where 6 equilibria are at play. The interactions of the Aβ(1-40) peptide and the porphyrins lead to nuclei, the formation of which is faster and/or more favored than in absence of porphyrin (Scheme 1.B versus Scheme 4, Eq. 1). This may be due to the fact that the porphyrins help several peptides to be gathered and/or to be oriented in a way more favorable for the self-assembly. As a reminder, several peptides are required to host one porphyrin, with ratio values that depend on the size of the porphyrin (Scheme 3). Then, two elongation paths may co-exist: (i) the first one where Aβ(1-40) is added at the extremities of the nucleus. Because the nuclei are different from those obtained in absence of porphyrins, they may be more prone to elongate (Eq. 2); (ii) the second one (Eq.3) where the addition of Aβ(1-40) at the extremities is promoted by the presence of the porphyrins. Eq. 2 and 3 contribute to the faster elongation rate observed in presence of cationic porphyrins (Figures 6 and S2) up to about the C_M concentration. Note that the interaction of the cationic porphyrins with assemblies of 4 to 5 peptides probed by the decrease of their intrinsic fluorescence and that precedes the formation of ThT-responsive fibrils may correspond to the formation of nuclei (Eq. 1). In addition, the higher the porphyrin concentration is, the shorter the time difference between the formation of nuclei and of ThT-responsive fibrils is (Figure 4). Considering that porphyrin fluorescence probes the formation of nuclei, such a concentration dependent trend may indicate that Eq. 3 (dependent on porphyrin concentration) contributes more to the whole assembly process than Eq. 2. (independent of porphyrin concentration). Porphyrins interaction with formed fibrils can also occur (Eq. 4). Note that, in this case, we cannot rule out that they substitute ThT in its binding site (as will be described later on for H_2-TMPyP). Eq. 1 to 4 are responsible for the shorter $t_{1/2}$ observed in the presence of porphyrins compared

View Article Online
DOI: 10.1039/D6QI00446F

to the apo Aβ(1-40) although modifications of secondary nucleation processes may also participate.[17-23] Last, Eq. 5 and 6 correspond to the filling of a second lower-affinity site in the nuclei that may correspond to the ThT binding site[86],[87] (Eq. 5) and to the further formation of off-pathways aggregates not detected by TEM and responsible for the ThT fluorescence loss (Eq. 6). The bulkiness of the **MA** family porphyrins prevent the formation of the cross-β sheet structure of the fibrils.[88, 89] Indeed, they are expected to insert into the groove made by hydrophobic residues involved in the inter-strand formation perpendicular to the axis fibrils.[90] As the distance between two strands is 11 Å, this does not leave enough space for **MA** insertion without disrupting the inter-strand peptide interaction (Scheme S2). The threshold value for which the concentration of porphyrin leads to the maximal fastening effect mainly corresponds to the balance between two factors: (i) the fastening effect previously described (Eq.1 – 4), higher for **Au-MA** versus **H_2-MA** and **Cu-MA** and (ii) the formation of off-pathways aggregates (Eq. 5 and 6).

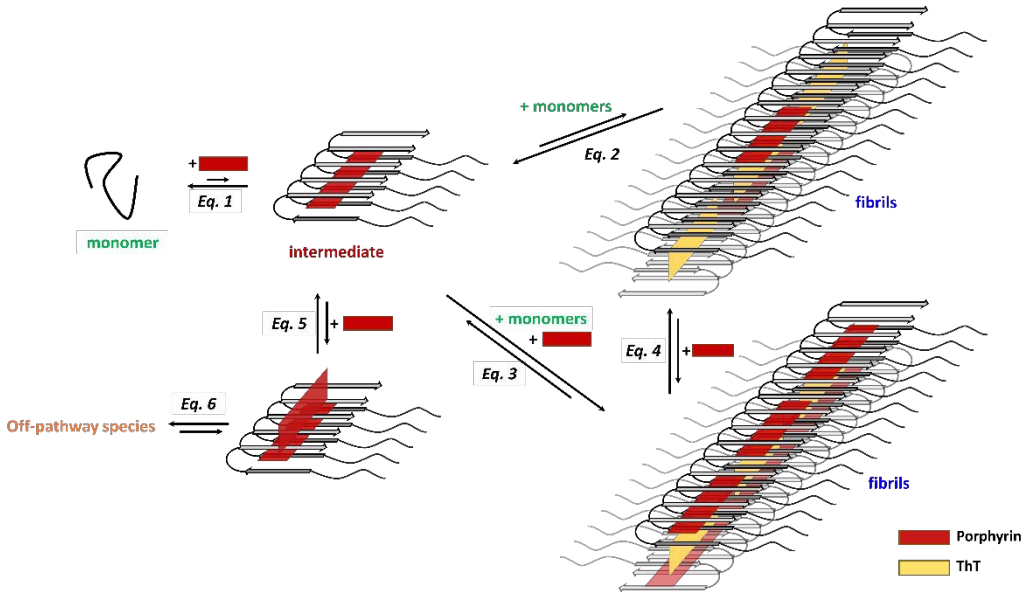

Scheme 4. Simplified mechanism to explain the effect of the **MA** family porphyrins on Aβ(1-40) self-assembly. Red rectangle = porphyrin and yellow rectangle = ThT.

For the **H_2-TMPyP** and **Au-TMPyP** (scheme S3), the preference for binding to site 1 (Eq. 1, and thus Eq. 2 – 4) versus site 2 (Eq. 5) is weaker than for the **MA** porphyrins, in line with a weaker fastening of Aβ(1-40) self-assembly. In addition, Eq. 5 can exist without leading to off-pathway aggregates because the **H_2-TMPyP** is smaller and can insert between the strands leading to 2 **H_2-TMPyP** per 4 peptides into the fibrils (Scheme S2) as shown by the detection in TEM and AFM of fibrils even for 10µM of **H_2-TMPyP** (Figures 1-6, S6, S7, S19). In this case, the decrease observed in the maximal ThT intensity can be explained by the removal of the ThT out of its interaction site that corresponds to the second site of the porphyrin (Scheme S2).[91]

View Article Online
DOI: 10.1039/D6QI00446F

6 –Concluding remarks

In the present article, we report on the concentration-dependent effect of a wide series of porphyrins on the Aβ(1-40) self-assembly. We propose a structure-activity relationship (SAR), in which the nature of porphyrin (charge, size and metal ions inserted) is key for the modulation of the Aβ(1-40) self-assembly. The various interactions are of different extents, with electrostatic forces being more important than hydrophobic and/or π-stacking ones (no effect of the anionic porphyrins in contrast to the cationic porphyrins). The size of the porphyrin is also crucial. In the case of the **H_2-TMPyP**, the fibrils can host two porphyrins per four peptides into two different binding sites. In the case of the bulkier **MA** porphyrins, only the first site is filled with a porphyrin: peptides ratio that cannot exceed 1:5 based on geometrical constraints while the filling of the second site leads to the formation of off-pathways aggregates. Fastening of the self-assembly is due to the preferential binding of the porphyrins into the first site where they gather and/or structure several peptides, more favored for **MA** compared to **H_2-TMPyP**. No coordination interaction was observed for the chosen metalated porphyrins, in line with the absence of apical binding site. Metalation of the porphyrins with Au(III), in contrast to with Cu(II), induces a stronger accelerating effects of the Aβ(1-40) self-assembly, due to higher charge and hydrophobicity.

Most studies related to modulation of amyloid-forming assembly have focused on porphyrins at a single molar equivalent, thus overlooking concentration dependent behaviours.[35, 37, 38, 41, 43-46, 53, 64, 65, 92, 93] When concentration studies were conducted a slowdown in kinetics, accompanied by inhibition of the self-assembly has been reported.[39, 42, 47] In contrast, we have evidenced here that the ratio between the porphyrin and the peptides is a crucial parameter to guide the modulatory effect on the Aβ(1-40) self-assembly. At low ratio (< 0.1 equiv. porphyrin versus peptide) a fastening effect is observed and at higher ratio the inhibition of fibril formation is detected for the **MA** series. We thus pointed out that beyond the nature of the modulator, the ratio with respect to the targeted peptide has also to be tightly controlled. Beyond porphyrins, only a few studies report the dependence of the Aβ(1-40)/Aβ(1-42) self-assembly as a function of a large range of modulators concentrations,[94-96] and a unique other case of a biphasic trend was described.[94]

In light of the results found in the present article, the interaction of heme with Aβ that attracted much attention might be revisited. Heme has been found to co-localize with Aβ plaques in the cerebral cortex of post-mortem AD brains and was early shown to inhibit Aβ aggregation.[35, 37, 38] The best characterized interaction of heme with Aβ peptides so far is its coordination with the His residues,[49, 50] which has not been detected here since Cu(II) and Au(III)-substituted porphyrins have no apical ligation site. From studies with mutated Aβ(1-40), residues Phe19 and Phe20 were both shown to be involved in the interaction of heme with Aβ(1-40),[36] as also detected here. However

View Article Online
DOI: 10.1039/D6QI00446F

rather than a 1:1 (Heme:Aβ(1-40)) species as currently described,[36, 50, 97-100] one may consider different interaction ratios in line with our concentration-dependent study.

Last but not least, the quest for Aβ assembly modulators, beyond the insights it can bring into a better understanding of the Aβ assembly itself, is justified by the still needed therapeutic options to control the deleterious assembly process. Here we have identified molecular important features and provided a coherent mechanism of action evidencing that not only the chemical nature of the modulator but also its ratio versus peptide matters. Among the key factors at play, the importance of the overall charge of the peptide versus the porphyrin is currently being confirmed by the study on positively charged peptides. It would be of high interest to confirm the importance of the overall charge of the peptide versus the porphyrin by the study on positively charged peptides as well as to decipher the role of apical ligation as anticipated based on the interaction of Heme with Aβ.

View Article Online
DOI: 10.1039/D6QI00446F

Acknowledgments

The authors acknowledge Lucie de Cremoux for the recording of the TEM images, David Schmidt for his help in the kinetic data automated mathematical treatment and the all-research team for fruitful discussions. We acknowledge the METi imaging facility, member of the national infrastructure France-BioImaging supported by the French National Research Agency (ANR-10-INBS-04). We acknowledge financial support from the ANR-16-CE18-0022 (project DIVA), ANR-22-CE44-0002-02 (project MASAI), and ANR-21-CE06-0030-01 (project SUPRAMY).

Abbreviations

AD, Alzheimer's disease; Aβ, amyloid β peptide; CHC, central hydrophobic core; SAR, structure activity relationship; ThT, thioflavin T; Tyr, tyrosine; EDTA, ethylenediaminetetraacetic acid; a.u, arbitrary units; TEM, transmission electron microscopy; AFM, atomic force microscopy; NMR, nuclear magnetic resonance; C_M, concentration threshold; ε, molar extinction coefficient; DNA, deoxyribonucleic acid; Val, valine; Phe, phenylalanine; His, histidine; Me, methyl; Met, methionine; Au, gold; Cu, copper; Ala, alanine; Leu, leucine; Eq, equilibrium.

References

1. Wells, C.; Brennan, S.; Keon, M.; Ooi, L., The role of amyloid oligomers in neurodegenerative pathologies. *Int. J. Biol. Macromol.* **2021,** *181*, 582-604.
2. Iadanza, M. G.; Jackson, M. P.; Hewitt, E. W.; Ranson, N. A.; Radford, S. E., A new era for understanding amyloid structures and disease. *Nat. Rev. Mol. Cell Biol.* **2018,** *19* (12), 755-773.
3. Almeida, Z. L.; Brito, R. M. M., Structure and Aggregation Mechanisms in Amyloids. *Molecules* **2020,** *25* (5), 1195.
4. Ke, P. C.; Sani, M.-A.; Ding, F.; Kakinen, A.; Javed, I.; Separovic, F.; Davis, T. P.; Mezzenga, R., Implications of peptide assemblies in amyloid diseases. *Chem. Soc. Rev.* **2017,** *46* (21), 6492-6531.
5. Ke, P. C.; Zhou, R.; Serpell, L. C.; Riek, R.; Knowles, T. P. J.; Lashuel, H. A.; Gazit, E.; Hamley, I. W.; Davis, T. P.; Fändrich, M.; Otzen, D. E.; Chapman, M. R.; Dobson, C. M.; Eisenberg, D. S.; Mezzenga, R., Half a century of amyloids: past, present and future. *Chemical Society Reviews* **2020,** *49* (15), 5473-5509.
6. Selkoe, D. J.; Hardy, J., The amyloid hypothesis of Alzheimer's disease at 25 years. *EMBO Mol. Med.* **2016,** *8* (6), 595-608.
7. Zhang, Y.; Chen, H.; Li, R.; Sterling, K.; Song, W., Amyloid β-based therapy for Alzheimer's disease: challenges, successes and future. *Sig. Transduct. Target. Ther.* **2023,** *8* (1), 248.
8. Monteiro, A. R.; Barbosa, D. J.; Remião, F.; Silva, R., Alzheimer's disease: Insights and new prospects in disease pathophysiology, biomarkers and disease-modifying drugs. *Biochem. Pharmacol.* **2023,** *211*, 115522.
9. Kim, B.-H.; Kim, S.; Nam, Y.; Park, Y. H.; Shin, S. M.; Moon, M., Second-generation anti-amyloid monoclonal antibodies for Alzheimer's disease: current landscape and future perspectives. *Trans. Neurodegen.* **2025,** *14* (1), 6.
10. Jucker, M.; Walker, L. C., Alzheimer's disease: From immunotherapy to immunoprevention. *Cell* **2023,** *186* (20), 4260-4270.

11. Atrián-Blasco, E.; Gonzalez, P.; Santoro, A.; Alies, B.; Faller, P.; Hureau, C., Cu and Zn coordination to amyloid peptides: From fascinating chemistry to debated pathological relevance. *Coord. Chem. Rev.* **2018,** *375*, 38-55.
12. Hureau, C., Chapter 7 Role of Metal Ions in Alzheimer's Disease: Mechanistic Aspects Contributing to Neurotoxicity. In *Alzheimer's Disease: Recent Findings in Pathophysiology, Diagnostic and Therapeutic Modalities*, Govindaraju, T., Ed. The Royal Society of Chemistry: 2022; pp 170-192.
13. Marshall, K. E.; Morris, K. L.; Charlton, D.; O'Reilly, N.; Lewis, L.; Walden, H.; Serpell, L. C., Hydrophobic, Aromatic, and Electrostatic Interactions Play a Central Role in Amyloid Fibril Formation and Stability. *Biochemistry* **2011,** *50* (12), 2061-2071.
14. Enache, T. A.; Chiorcea-Paquim, A.-M.; Oliveira-Brett, A. M., Amyloid Beta Peptide VHHQ, KLVFF, and IIGLMVGGVV Domains Involved in Fibrilization: AFM and Electrochemical Characterization. *Anal. Chem.* **2018,** *90* (3), 2285-2292.
15. Reiss, A. B.; Arain, H. A.; Stecker, M. M.; Siegart, N. M.; Kasselman, L. J., Amyloid toxicity in Alzheimer's disease. *Rev. Neurosci.* **2018,** *29* (6), 613-627.
16. Rana, M.; Sharma, A. K., Cu and Zn interactions with Aβ peptides: consequence of coordination on aggregation and formation of neurotoxic soluble Aβ oligomers. *Metallomics* **2018,** *11* (1), 64-84.
17. Törnquist, M.; Michaels, T. C. T.; Sanagavarapu, K.; Yang, X.; Meisl, G.; Cohen, S. I. A.; Knowles, T. P. J.; Linse, S., Secondary nucleation in amyloid formation. *Chem. Commun.* **2018,** *54* (63), 8667-8684.
18. Linse, S., Toward the equilibrium and kinetics of amyloid peptide self-assembly. *Curr. Opin. Struct. Biol.* **2021,** *70*, 87-98.
19. Meisl, G.; Knowles, T. P. J.; Klenerman, D., Mechanistic Models of Protein Aggregation Across Length-Scales and Time-Scales: From the Test Tube to Neurodegenerative Disease. *Frontiers in neuroscience* **2022,** *16*.
20. Faller, P.; Hureau, C., Reproducibility Problems of Amyloid-β Self-Assembly and How to Deal With Them. *Front.Chem.* **2021,** *8*.
21. Lee, S. J. C.; Nam, E.; Lee, H. J.; Savelieff, M. G.; Lim, M. H., Towards an understanding of amyloid-β oligomers: characterization, toxicity mechanisms, and inhibitors. *Chem. Soc. Rev.* **2017,** *46* (2), 310-323.
22. Linse, S., Monomer-dependent secondary nucleation in amyloid formation. *Biophys. Rev.* **2017,** *9* (4), 329-338.
23. Srivastava, A. K.; Pittman, J. M.; Zerweck, J.; Venkata, B. S.; Moore, P. C.; Sachleben, J. R.; Meredith, S. C., β-Amyloid aggregation and heterogeneous nucleation. *Protein Sci.* **2019,** *28* (9), 1567-1581.
24. Bieschke, J.; Herbst, M.; Wiglenda, T.; Friedrich, R. P.; Boeddrich, A.; Schiele, F.; Kleckers, D.; Lopez del Amo, J. M.; Grüning, B. A.; Wang, Q.; Schmidt, M. R.; Lurz, R.; Anwyl, R.; Schnoegl, S.; Fändrich, M.; Frank, R. F.; Reif, B.; Günther, S.; Walsh, D. M.; Wanker, E. E., Small-molecule conversion of toxic oligomers to nontoxic β-sheet–rich amyloid fibrils. *Nat. Chem. Biol.* **2012,** *8* (1), 93-101.
25. Habchi, J.; Chia, S.; Limbocker, R.; Mannini, B.; Ahn, M.; Perni, M.; Hansson, O.; Arosio, P.; Kumita, J. R.; Challa, P. K.; Cohen, S. I. A.; Linse, S.; Dobson, C. M.; Knowles, T. P. J.; Vendruscolo, M., Systematic development of small molecules to inhibit specific microscopic steps of Aβ42 aggregation in Alzheimer's disease. *Proc. Natl. Acad. Sci. USA* **2017,** *114* (2), E200-E208.
26. Maity, D., Inhibition of Amyloid Protein Aggregation Using Selected Peptidomimetics. *ChemMedChem* **2023,** *18* (2), e202200499.
27. Maity, D., Recent advances in the modulation of amyloid protein aggregation using the supramolecular host-guest approaches. *Biophysical Chemistry* **2023,** *297*, 107022.
28. Roy, R.; Paul, S., Illustrating the Effect of Small Molecules Derived from Natural Resources on Amyloid Peptides. *The Journal of Physical Chemistry B* **2023,** *127* (3), 600-615.
29. Perneczky, R.; Jessen, F.; Grimmer, T.; Levin, J.; Flöel, A.; Peters, O.; Froelich, L., Anti-amyloid antibody therapies in Alzheimer's disease. *Brain* **2023,** *146* (3), 842-849.

30. Shao, X.; Yan, C.; Wang, C.; Wang, C.; Cao, Y.; Zhou, Y.; Guan, P.; Hu, X.; Zhu, W.; Ding, S., Advanced nanomaterials for modulating Alzheimer's related amyloid aggregation. *Nanoscale Advances* **2023,** *5* (1), 46-80.
31. Gomes, L. M. F.; Bataglioli, J. C.; Storr, T., Metal complexes that bind to the amyloid-β peptide of relevance to Alzheimer's disease. *Coord. Chem. Rev.* **2020,** *412*, 213255.
32. Yoo, J.; Lee, J.; Ahn, B.; Han, J.; Lim, M. H., Multi-target-directed therapeutic strategies for Alzheimer's disease: controlling amyloid-β aggregation, metal ion homeostasis, and enzyme inhibition. *Chem. Sci.* **2025,** *16* (5), 2105-2135.
33. Fan, Y.; Wu, D.; Yi, X.; Tang, H.; Wu, L.; Xia, Y.; Wang, Z.; Liu, Q.; Zhou, Z.; Wang, J., TMPyP Inhibits Amyloid-beta Aggregation and Alleviates Amyloid-Induced Cytotoxicity. *ACS Omega* **2017,** *2* (8), 4188-4195.
34. Lee, B. I.; Lee, S.; Suh, Y. S.; Lee, J. S.; Kim, A. K.; Kwon, O. Y.; Yu, K.; Park, C. B., Photoexcited Porphyrins as a Strong Suppressor of beta-Amyloid Aggregation and Synaptic Toxicity. *Angew. Chem. Int. Ed.* **2015,** *54* (39), 11472-11476.
35. Howlett, D.; Cutler, P.; Heales, S.; Camilleri, P., Hemin and related porphyrins inhibit beta-amyloid aggregation. *FEBS Lett.* **1997,** *417* (2), 249-251.
36. Yuan, C.; Gao, Z., Abeta interacts with both the iron center and the porphyrin ring of heme: mechanism of heme's action on Abeta aggregation and disaggregation. *Chem. Res. Toxicol.* **2013,** *26* (2), 262-269.
37. Taniguchi, S.; Suzuki, N.; Masuda, M.; Hisanaga, S.; Iwatsubo, T.; Goedert, M.; Hasegawa, M., Inhibition of heparin-induced tau filament formation by phenothiazines, polyphenols, and porphyrins. *J. Biol. Chem.* **2005,** *280* (9), 7614-7623.
38. Masuda, M.; Suzuki, N.; Taniguchi, S.; Oikawa, T.; Nonaka, T.; Iwatsubo, T.; Hisanaga, S.; Goedert, M.; Hasegawa, M., Small molecule inhibitors of alpha-synuclein filament assembly. *Biochemistry* **2006,** *45* (19), 6085-6094.
39. Dong, C.; Garen, C. R.; Mercier, P.; Petersen, N. O.; Woodside, M. T., Characterizing the inhibition of α-synuclein oligomerization by a pharmacological chaperone that prevents prion formation by the protein PrP. *Protein Science* **2019,** *28* (9), 1690-1702.
40. González, N.; Gentile, I.; Garro, H. A.; Delgado-Ocaña, S.; Ramunno, C. F.; Buratti, F. A.; Griesinger, C.; Fernández, C. O., Metal coordination and peripheral substitution modulate the activity of cyclic tetrapyrroles on αS aggregation: a structural and cell-based study. *J. Biol. Inorg. Chem.* **2019,** *24* (8), 1269-1278.
41. Fonseca-Ornelas, L.; Eisbach, S. E.; Paulat, M.; Giller, K.; Fernández, C. O.; Outeiro, T. F.; Becker, S.; Zweckstetter, M., Small molecule-mediated stabilization of vesicle-associated helical α-synuclein inhibits pathogenic misfolding and aggregation. *Nat. Commun.* **2014,** *5* (1), 5857.
42. Nath, S.; Roy, P.; Mandal, R.; Roy, R.; Buell, A. K.; Sengupta, N.; Tarafdar, P. K., Hydroxy-Porphyrin as an Effective, Endogenous Molecular Clamp during Early Stages of Amyloid Fibrillization. *Chem. Asian J.* **2021,** *16* (23), 3931-3936.
43. Chernii, S.; Losytskyy, M.; Kelm, A.; Gorski, A.; Tretyakova, I.; Yarmoluk, S.; Chernii, V.; Kovalska, V., Study of tetraphenylporphyrins as modifiers of insulin amyloid aggregation. *J. Mol. Recognit.* **2020,** *33* (1), e2811.
44. Wu, J.; Zhao, J.; Yang, Z.; Li, H.; Gao, Z., Strong Inhibitory Effect of Heme on hIAPP Fibrillation. *Chem. Res. Toxicol.* **2017,** *30* (9), 1711-1719.
45. Zhang, P.; Zeng, L.; Gao, W.; Li, H.; Gao, Z., Peroxynitrite scavenger FeTPPS effectively inhibits hIAPP aggregation and protects against amyloid induced cytotoxicity. *Int. J. Biol. Macromol.* **2020,** *161*, 336-344.
46. Wu, J.; Yin, X.; Ye, H.; Gao, Z.; Li, H., Structure relationship of metalloporphyrins in inhibiting the aggregation of hIAPP. *Int. J. Biol. Macromol.* **2021,** *167*, 141-150.
47. Zhou, X.; Zhang, L.; Zhi, J.; Zhao, L.; Shen, R.; Yang, A.; Kou, X., Zinc-porphyrin complex as multifunctional anti-AD agent: Synthesis, X-ray single crystal analysis and activity study. *J. Inorg. Biochem.* **2026**, 113245.

View Article Online
DOI: 10.1039/D6QI00446F

48. Dey, C.; Roy, M.; Pal, P.; Ghosh, R.; Dey, S. G., Mechanism of oxidative stress and neurotoxicity associated with heme and copper–Aβ relevant to Alzheimer's disease. *Chem. Soc. Rev.* **2025,** *54* (20), 9457-9499.
49. Poulos, T. L., Heme Enzyme Structure and Function. *Chem. Rev.* **2014,** *114* (7), 3919-3962.
50. Roy, M.; Nath, A. K.; Pal, I.; Dey, S. G., Second Sphere Interactions in Amyloidogenic Diseases. *Chem. Rev.* **2022,** *122* (14), 12132-12206.
51. Pal, I.; Dey, S. G., The Role of Heme and Copper in Alzheimer's Disease and Type 2 Diabetes Mellitus. *JACS Au* **2023,** *3* (3), 657-681.
52. Villari, V.; Tosto, R.; Di Natale, G.; Sinopoli, A.; Tomasello, M. F.; Lazzaro, S.; Micali, N.; Pappalardo, G., A Metalloporphyrin-Peptide Conjugate as an Effective Inhibitor of Amyloid-β Peptide Fibrillation and Cytotoxicity. *ChemistrySelect* **2017,** *2* (28), 9122-9129.
53. Xu, W.; Gao, C.; Sun, X.; Tai, W. C.-S.; Lung, H. L.; Law, G.-L., Design, synthesis and comparison of water-soluble phthalocyanine/porphyrin analogues and their inhibition effects on Aβ42 fibrillization. *Inorg. Chem. Front.* **2021,** *8* (14), 3501-3513.
54. Wang, L.; Eom, K.; Kwon, T., Different Aggregation Pathways and Structures for Aβ40 and Aβ42 Peptides. *Biomolecules* **2021,** *11* (2), 198.
55. Meisl, G.; Yang, X.; Hellstrand, E.; Frohm, B.; Kirkegaard, J. B.; Cohen, S. I. A.; Dobson, C. M.; Linse, S.; Knowles, T. P. J., Differences in nucleation behavior underlie the contrasting aggregation kinetics of the Aβ40 and Aβ42 peptides. *Proc. Natl. Acad. Sci. U. S. A.* **2014,** *111* (26), 9384-9389.
56. Romera, C.; Sabater, L.; Garofalo, A.; I, M. D.; Pratviel, G., Interaction of cationic nickel and manganese porphyrins with the minor groove of DNA. *Inorg. Chem.* **2010,** *49* (18), 8558-8567.
57. Pipier, A.; De Rache, A.; Modeste, C.; Amrane, S.; Mothes-Martin, E.; Stigliani, J.-L.; Calsou, P.; Mergny, J.-L.; Pratviel, G.; Gomez, D., G-Quadruplex binding optimization by gold(III) insertion into the center of a porphyrin. *Dalton Trans.* **2019,** *48* (18), 6091-6099.
58. Dobrovodsky, D.; Danhel, A.; Mothes-Martin, E.; Pratviel, G.; Mergny, J.-L.; Fojta, M., Voltammetric studies of selected porphyrin G-quadruplex ligands and their interaction with DNA in solution and at the mercury electrode surface. *Electrochim. Acta* **2021,** *394*, 139151.
59. Conte-Daban, A.; Ambike, V.; Guillot, R.; Delsuc, N.; Policar, C.; Hureau, C., A Metallo Pro-Drug to Target Cu(II) in the Context of Alzheimer's Disease. *Chem. Eur. J.* **2018,** *24* (20), 5095-5099.
60. de Cremoux, L.; Falcone, E.; Schmitt, D.; Stefaniak, E.; Wiśniewska, M. D.; Vitale, N.; Bal, W.; Hureau, C., Modulation of Aβ1–40 and Aβ4–40 co-assembly by zinc: getting closer to the biological reality. *Inorg. Chem. Front.* **2025,** *12* (23), 7827-7844.
61. Faller, P.; Hureau, C.; Dorlet, P.; Hellwig, P.; Coppel, Y.; Collin, F.; Alies, B., Methods and techniques to study the bioinorganic chemistry of metal–peptide complexes linked to neurodegenerative diseases. *Coord. Chem. Rev.* **2012,** *256* (19), 2381-2396.
62. Conte-Daban, A.; Day, A.; Faller, P.; Hureau, C., How Zn can impede Cu detoxification by chelating agents in Alzheimer's disease: a proof-of-concept study. *Dalton Trans.* **2016,** *45* (39), 15671-15678.
63. Dixon, I. M.; Lopez, F.; Tejera, A. M.; Esteve, J. P.; Blasco, M. A.; Pratviel, G.; Meunier, B., A G-quadruplex ligand with 10000-fold selectivity over duplex DNA. *J. Am. Chem. Soc.* **2007,** *129* (6), 1502-1503.
64. Zhang, Q.; Liu, Y.; Wu, J.; Zeng, L.; Wei, J.; Fu, S.; Ye, H.; Li, H.; Gao, Z., Structure and mechanism behind the inhibitory effect of water soluble metalloporphyrins on Aβ1–42 aggregation. *Inorg. Chem. Front.* **2022,** *9* (7), 1520-1532.
65. Kovalska, V.; Chernii, S.; Losytskyy, M.; Ostapko, J.; Tretyakova, I.; Gorski, A.; Chernii, V.; Yarmoluk, S., Activity of Zn and Mg phthalocyanines and porphyrazines in amyloid aggregation of insulin. *J. Mol. Recognit.* **2018,** *31* (1), e2660.
66. Shoffner, S. K.; Schnell, S., Estimation of the lag time in a subsequent monomer addition model for fibril elongation. *Phys. Chem. Chem. Phys.* **2016,** *18* (31), 21259-21268.
67. Stefaniak, E.; Atrian-Blasco, E.; Goch, W.; Sabater, L.; Hureau, C.; Bal, W., The Aggregation Pattern of Aβ1–40 is Altered by the Presence of N-Truncated Aβ4–40 and/or CuII in a Similar Way through Ionic Interactions. *Chem. Eur. J.* **2021,** *27* (8), 2798-2809.

68. Tian, Y.; Viles, J. H., pH Dependence of Amyloid-β Fibril Assembly Kinetics: Unravelling the Microscopic Molecular Processes. *Angew. Chem. Int. Ed.* **2022,** *61* (48), e202210675.
69. Wheelhouse, R. T.; Sun, D.; Han, H.; Han, F. X.; Hurley, L. H., Cationic Porphyrins as Telomerase Inhibitors: the Interaction of Tetra-(N-methyl-4-pyridyl)porphine with Quadruplex DNA. *J. Am. Chem. Soc.* **1998,** *120* (13), 3261-3262.
70. Kelly, J. M.; Murphy, M. J.; McConnell, D. J.; OhUigin, C., A comparative study of the interaction of 5,10,15,20-tetrakis (N-methylpyridinium-4-yl)porphyrin and its zinc complex with DNA using fluorescence spectroscopy and topoisomerisation. *Nucleic Acids Res.* **1985,** *13* (1), 167-184.
71. Teixeira, R.; Serra, V. V.; Botequim, D.; Paulo, P. M. R.; Andrade, S. M.; Costa, S. M. B. Fluorescence Spectroscopy of Porphyrins and Phthalocyanines: Some Insights into Supramolecular Self-Assembly, Microencapsulation, and Imaging Microscopy *Molecules* [Online], 2021.
72. Bohandy, J.; Kim, B., F. In *SPECTROSCOPY OF PORPHYRINS*, Digest, J. H. A. T., Ed. 1981.
73. Zakavi, S.; Hoseini, S., The absorption and fluorescence emission spectra of meso-tetra(aryl)porphyrin dications with weak and strong carboxylic acids: a comparative study. *RSC Adv.* **2015,** *5* (129), 106774-106786.
74. Vivekanandan, S.; Brender, J. R.; Lee, S. Y.; Ramamoorthy, A., A partially folded structure of amyloid-beta(1–40) in an aqueous environment. *Biochemical and Biophysical Research Communications* **2011,** *411* (2), 312-316.
75. Danielsson, J.; Pierattelli, R.; Banci, L.; Graslund, A., High-resolution NMR studies of the zinc-binding site of the Alzheimer's amyloid beta-peptide. *FEBS Journal* **2007,** *274* (1), 46-59.
76. Hou, L.; Shao, H.; Zhang, Y.; Li, H.; Menon, N. K.; Neuhaus, E. B.; Brewer, J. M.; Byeon, I. J.; Ray, D. G.; Vitek, M. P.; Iwashita, T.; Makula, R. A.; Przybyla, A. B.; Zagorski, M. G., Solution NMR studies of the A beta(1-40) and A beta(1-42) peptides establish that the Met35 oxidation state affects the mechanism of amyloid formation. *J. Am. Chem. Soc.* **2004,** *126* (7), 1992-2005.
77. Wahlström, A.; Cukalevski, R.; Danielsson, J.; Jarvet, J.; Onagi, H.; Rebek, J., Jr.; Linse, S.; Gräslund, A., Specific Binding of a β-Cyclodextrin Dimer to the Amyloid β Peptide Modulates the Peptide Aggregation Process. *Biochemistry* **2012,** *51* (21), 4280-4289.
78. Wallin, C.; Jarvet, J.; Biverstål, H.; Wärmländer, S.; Danielsson, J.; Gräslund, A.; Abelein, A., Metal ion coordination delays amyloid-β peptide self-assembly by forming an aggregation–inert complex. *Journal of Biological Chemistry* **2020,** *295* (21), 7224-7234.
79. Briggs, B. N.; Gaier, A. J.; Fanwick, P. E.; Dogutan, D. K.; McMillin, D. R., Cationic Copper(II) Porphyrins Intercalate into Domains of Double-Stranded RNA. *Biochemistry* **2012,** *51* (38), 7496-7505.
80. Li, J.; Wei, Y.; Guo, L.; Zhang, C.; Jiao, Y.; Shuang, S.; Dong, C., Study on spectroscopic characterization of Cu porphyrin/Co porphyrin and their interactions with ctDNA. *Talanta* **2008,** *76* (1), 34-39.
81. Kadish, K. M.; Smith, K. M.; Guilard, R., *The porphyrin handbook. Vol. 3, Inorganic, organometallic and coordination chemistry*. Academic San Diego, Calif.: San Diego, Calif., 2000.
82. Fleischer, E. B., Structure of porphyrins and metalloporphyrins. *Acc. Chem. Res.* **1970,** *3* (3), 105-112.
83. Köhler, F. H., Paramagnetic Complexes in Solution: The NMR Approach. In *eMagRes*.
84. Hureau, C.; Dorlet, P., Coordination of redox active metal ions to the APP protein and to the amyloid-β peptides involved in Alzheimer disease. Part 2: How Cu(II) binding sites depend on changes in the Aβ sequences. . *Coord. Chem. Rev.* **2012,** *256* (19-20), 2175-2187.
85. Jumper, J.; Evans, R.; Pritzel, A.; Green, T.; Figurnov, M.; Ronneberger, O.; Tunyasuvunakool, K.; Bates, R.; Žídek, A.; Potapenko, A.; Bridgland, A.; Meyer, C.; Kohl, S. A. A.; Ballard, A. J.; Cowie, A.; Romera-Paredes, B.; Nikolov, S.; Jain, R.; Adler, J.; Back, T.; Petersen, S.; Reiman, D.; Clancy, E.; Zielinski, M.; Steinegger, M.; Pacholska, M.; Berghammer, T.; Bodenstein, S.; Silver, D.; Vinyals, O.; Senior, A. W.; Kavukcuoglu, K.; Kohli, P.; Hassabis, D., Highly accurate protein structure prediction with AlphaFold. *Nature* **2021,** *596* (7873), 583-589.
86. Biancalana, M.; Koide, S., Molecular mechanism of Thioflavin-T binding to amyloid fibrils. *BBA Proteins and Proteomics* **2010,** *1804* (7), 1405-1412.

87. Reinke, A. A.; Gestwicki, J. E., Insight into Amyloid Structure Using Chemical Probes. *Chem. Biol. Drug Des.* **2011,** *77* (6), 399-411.
88. Sabaté, R.; Ventura, S., Cross-β-Sheet Supersecondary Structure in Amyloid Folds: Techniques for Detection and Characterization. In *Protein Supersecondary Structures*, Kister, A. E., Ed. Humana Press: Totowa, NJ, 2013; pp 237-257.
89. Riek, R., The Three-Dimensional Structures of Amyloids. *Cold Spring Harbor Perspectives in Biology* **2017,** *9*.
90. Noël, S.; Cadet, S.; Gras, E.; Hureau, C., The benzazole scaffold: a SWAT to combat Alzheimer's Disease. *Chem. Soc. Rev.* **2013,** *42*, 7747-7762.
91. Sulatskaya, A. I.; Rychkov, G. N.; Sulatsky, M. I.; Mikhailova, E. V.; Melnikova, N. M.; Andozhskaya, V. S.; Kuznetsova, I. M.; Turoverov, K. K., New Evidence on a Distinction between Aβ40 and Aβ42 Amyloids: Thioflavin T Binding Modes, Clustering Tendency, Degradation Resistance, and Cross-Seeding. *Int. J. Mol. Sci.* **2022,** *23* (10), 5513.
92. Li, M.; Zhao, A.; Ren, J.; Qu, X., N-Methyl Mesoporphyrin IX as an Effective Probe for Monitoring Alzheimer's Disease β-Amyloid Aggregation in Living Cells. *ACS Chem. Neurosci.* **2017,** *8* (6), 1299-1304.
93. Yuan, C.; Gao, Z., Aβ interacts with both the iron center and the porphyrin ring of heme: mechanism of heme's action on Aβ aggregation and disaggregation. *Chem. Res. Toxicol.* **2013,** *26*, 262.
94. Sahoo, B. R.; Genjo, T.; Nakayama, T. W.; Stoddard, A. K.; Ando, T.; Yasuhara, K.; Fierke, C. A.; Ramamoorthy, A., A cationic polymethacrylate-copolymer acts as an agonist for β-amyloid and an antagonist for amylin fibrillation. *Chemical Science* **2019,** *10* (14), 3976-3986.
95. Liu, F.; Zhao, W.; Zhao, F.; Dong, Q.; Wang, Y.; Wei, W.; Jia, L.; Li, L.; Lu, F., Dual Effect of the Acidic Polysaccharose Ulvan on the Inhibition of Amyloid-β Protein Fibrillation and Disintegration of Mature Fibrils. *ACS Appl. Mater. Interfaces* **2020,** *12* (37), 41167-41176.
96. Ramesh, M.; Acharya, A.; Murugan, N. A.; Ila, H.; Govindaraju, T., Thiophene-Based Dual Modulators of Aβ and Tau Aggregation. *ChemBioChem* **2021,** *22* (23), 3348-3357.
97. Pramanik, D.; Ghosh, C.; Dey, S. G., Heme–Cu Bound Aβ Peptides: Spectroscopic Characterization, Reactivity, and Relevance to Alzheimer's Disease. *J. Am. Chem. Soc.* **2011,** *133* (39), 15545-15552.
98. Thiabaud, G.; Pizzocaro, S.; Garcia-Serres, R.; Latour, J.-M.; Monzani, E.; Casella, L., Heme Binding Induces Dimerization and Nitration of Truncated β-Amyloid Peptide Aβ16 Under Oxidative Stress. *Angew. Chem. Int. Ed.* **2013,** *52* (31), 8041-8044.
99. Bacchella, C.; Brewster, J. T.; Bähring, S.; Dell'Acqua, S.; Root, H. D.; Thiabaud, G. D.; Reuther, J. F.; Monzani, E.; Sessler, J. L.; Casella, L., Condition-Dependent Coordination and Peroxidase Activity of Hemin-Aβ Complexes. *Molecules* **2020,** *25* (21), 5044.
100. Gout, J.; Meuris, F.; Desbois, A.; Dorlet, P., In vitro coordination of Fe-protoheme with amyloid beta is non-specific and exhibits multiple equilibria. *J. Inorg. Biochem.* **2022,** *227*, 111664.

The authors state that the data are available in the Supporting Information and on request from the corresponding author.

View Article Online
DOI: 10.1039/D6QI00446F